(19) Europäisches Patentamt
European Patent Office
Office européen des brevets

(11) **EP 3 470 329 B9**

(12) **CORRECTED EUROPEAN PATENT SPECIFICATION**

(15) Correction information:
Corrected version no 1 (W1 B1)
Corrections, see
Description Paragraph(s) 31

(48) Corrigendum issued on:
27.03.2024 Bulletin 2024/13

(45) Date of publication and mention of the grant of the patent:
17.01.2024 Bulletin 2024/03

(21) Application number: **17812924.3**

(22) Date of filing: **21.02.2017**

(51) International Patent Classification (IPC):
B64C 3/10 *(2006.01)* ***B64C 30/00*** *(2006.01)*

(52) Cooperative Patent Classification (CPC):
B64C 3/10; B64C 30/00; Y02T 50/10

(86) International application number:
PCT/JP2017/006404

(87) International publication number:
WO 2017/217015 (21.12.2017 Gazette 2017/51)

(54) **WING AND AIRCRAFT**

FLÜGEL UND FLUGZEUG

AILE ET AÉRONEF

(84) Designated Contracting States:
AL AT BE BG CH CY CZ DE DK EE ES FI FR GB GR HR HU IE IS IT LI LT LU LV MC MK MT NL NO PL PT RO RS SE SI SK SM TR

(30) Priority: **13.06.2016 JP 2016116898**

(43) Date of publication of application:
17.04.2019 Bulletin 2019/16

(73) Proprietor: **Japan Aerospace Exploration Agency**
Tokyo 182-8522 (JP)

(72) Inventors:
- **UEDA, Yoshine**
  Chofu-shi, Tokyo 182-8522 (JP)
- **TOKUGAWA, Naoko**
  Chofu-shi, Tokyo 182-8522 (JP)

(74) Representative: **Michalski Hüttermann & Partner Patentanwälte mbB**
Kaistraße 16A
40221 Düsseldorf (DE)

(56) References cited:
EP-A2- 2 466 288 JP-A- 2012 126 205

- **OLIVIER VERMEERSCH ET AL: "Natural laminar flow wing for supersonic conditions: Wind tunnel experiments, flight test and stability computations", PROGRESS IN AEROSPACE SCIENCES, vol. 79, 1 November 2015 (2015-11-01), pages 64-91, XP055645144, GB ISSN: 0376-0421, DOI: 10.1016/j.paerosci.2015.07.003**
- **YOSHINE UEDA ET AL: "Supersonic Natural-Laminar-Flow Wing-Design Concept at High-Reynolds-Number Conditions", AIAA JOURNAL, vol. 52, no. 6, 1 June 2014 (2014-06-01), pages 1294-1306, XP055645507, US ISSN: 0001-1452, DOI: 10.2514/1.J052555**

EP 3 470 329 B9

Description

Technical Field

[0001] The present invention relates to a wing to be used for an aircraft and the like and an aircraft including such a wing.

Background Art

[0002] It is an important problem to reduce drag in order to improve economic efficiency of aircrafts. Many aerodynamic design concepts for reducing pressure drag have been developed. Meanwhile, a beneficial concept for reducing friction drag in order to further reduce drag has not been produced.

[0003] In a swept-back wing, boundary layer transition is easily induced in the vicinity of a leading edge due to a physical mechanism called cross-flow instability (C-F instability). Therefore, it has been considered that it is difficult to realize natural laminarization over a wide range.

[0004] Yoshine UEDA, et al., inventors of the present invention, have proposed a natural laminarization-related technique of delaying the boundary layer transition on a wing surface to reduce friction drag (see Patent Literature 1).

[0005] That technique uses: a process of setting an initial shape of a cross-sectional wing shape; a CFD analysis process of determining pressure distribution of a flow-field in the vicinity of the cross-sectional wing shape obtained; a transition analysis process of estimating a boundary layer transition position on a wing surface; a process of setting target pressure distributions for wing upper and lower surfaces based on the pressure distribution; and a CFD-based inverse problem design process including the CFD analysis process and a shape correction process "correcting the cross-sectional wing shape such that the pressure distribution obtained from the CFD analysis process converges on the target pressure distribution." Moreover, the technique is as follows: in such a CFD-based inverse problem design process, among the target pressure distributions, the wing upper surface target pressure distribution defines "a wing chordwise direction from a wing leading edge to a wing trailing edge" as a domain at each spanwise station, and moreover is provided by a functional type with parameters dependent on the spanwise station as coefficients; then the sensitivity of the wing upper surface boundary layer transition due to fluctuations in each of the parameter values of the parameters is analyzed by the transition analysis process; and an optimal combination of parameter values that delays the wing upper surface boundary layer transition the furthest rearward at a desired Reynolds number is determined by performing a search.

Citation List

Patent Literature

[0006]

Patent Literature 1: Japanese Patent No. JP 5747343 B2. According to its abstract, this document discloses a method of designing a natural laminar flow wing which reduces friction drag by delaying boundary layer transition under flight conditions of actual aircrafts.

Non-Patent Literature 1: Olivier Vermeersch et al. describes "Natural laminar flow wing for supersonic conditions: Wind tunnel experiments, flight test and stability computations" in PROGRESS IN AEROSPACE SCIENCES, GB, vol. 79. According to its abstract, this document discloses a new natural laminar flow highly swept wing.

Non-Patent Literature 2: Yoshine Ueda et al. describe "Supersonic Natural-Laminar-Flow Wing-Design Concept at High-Reynolds-Number Conditions" in AIAA JOURNAL, US, vol. 52, no. 6. According to its abstract, this document discloses an effective method to create a new ideal pressure distribution for designing a three-dimensional natural-laminar-flow wing at high-Reynolds-number conditions to reduce friction drag of a large-size supersonic transport with 300 passengers.

Disclosure of Invention

Technical Problem

[0007] The above-mentioned technique uses the CFD-based inverse problem design process of determining the cross-sectional wing shape on the basis of the pressure distribution of the wing surface. It is necessary to determine independently each pressure distribution on the wing surfaces of the wing cross-sections such that components in an external

streamline direction of the wing surface (boundary between a viscous region and a potential region) and a cross-flow direction perpendicular thereto in each wing cross-section taken in the wingspan direction are reduced in the vicinity of the leading edge. Moreover, if any part of the cross-sectional wing shapes corresponding to the determined pressure distributions has insufficient performance, it can adversely affect the whole pressure distribution.

[0008] Therefore, it is very difficult just to make a design.

[0009] Moreover, even if a suitable design can be made, it is difficult to manufacture wings of an actual aircraft because the leading-edge shape of the wing shape based on such a design result is sharper toward the wing tip. It is because there are problems of deterioration of the structural strength and reduction of the working accuracy in manufacturing the wing having the leading-edge shape shaper toward the wing tip.

[0010] Further, high temperature due to heat generated by air compression and viscous friction near a stagnation point at a wing tip end affects the strength and the like of its structure. In a case of an existing wing having a small radius of curvature, there is also a problem that the rigidity of the aircraft body is lowered due to that frictional heat.

[0011] In view of the above-mentioned circumstances, it is an object of the present invention to provide a wing achieving reduction of friction drag and easy to design and also easy to manufacture and an aircraft including such a wing.

Solution to Problem

[0012] As to the above-mentioned problem, owing to development of a transition point prediction method in recent years, the instability of the boundary layer can be analyzed in a numerical analysis manner. An ideal pressure distribution suitable for natural laminarization can be obtained by grasping a relationship between a pressure distribution and transition by using the transition point prediction method. The inventors of the present invention found an optimal distribution form by displaying a pressure distribution form as a function and searching for configurations of parameters thereof. In addition, the inventors of the present invention determined a characteristic shape which can reproduce that pressure distribution.

[0013] The invention is defined by the features of the independent claim.

[0014] In the present invention, a flow in a direction opposite to that of the cross-flow component is induced by utilizing a difference between a rising pressure gradient at the wing root and a rising pressure gradient at the wing tip. In this manner, the cross-flow component can be reduced and the transition from the laminar flow to the turbulent flow can be suppressed. Moreover, an ideal pressure distribution suitable for natural laminarization is determined by grasping a relationship between a pressure distribution and transition by using a transition point prediction method, and its shape is also determined. Therefore, it is easy to make a design.

[0015] The wing according to the present invention can be used for the supersonic aircraft and the subsonic aircraft.

Advantageous Effects of Invention

[0016] In accordance with the present invention, cross-flow components in an external streamline direction of a wing surface and in a direction perpendicular thereto are reduced in the vicinity of the leading edge, and the boundary layer transition is not easily induced in the vicinity of the leading edge. With this, the friction drag caused by the cross-flow instability can be reduced. Furthermore, it is easy to design and also easy to manufacture it.

Brief Description of Drawings

[0017]

[Fig. 1] A top view of a wing as a main wing of an aircraft according to an embodiment of the present invention.
[Fig. 2] A cross-sectional view of the wing shown in Fig. 1, which is taken at an arbitrary position.
[Fig. 3] A diagram showing pressure distributions (Cp) on an upper surface of the vicinity of a leading edge of a wing (supersonic aircraft) according to the embodiment of the present invention.
[Fig. 4] A diagram showing pressure distributions (Cp) on the upper surface of the vicinity of the leading edge of the wing (supersonic aircraft) according to Patent Literature 1.
[Fig. 5] A diagram for describing parameters of a pressure distribution (Cp) according to the embodiment of the present invention.
[Fig. 6] A diagram showing a cross-sectional shape of an airfoil (supersonic aircraft) of the wing according to the embodiment of the present invention, which is non-dimensionalized.
[Fig. 7] An enlarged view of the vicinity of the leading edge of the cross-sectional shape shown in Fig. 6.
[Fig. 8] A graph showing a non-dimensional radius of curvature of the vicinity of the leading edge including both of an upper surface and a lower surface of the wing (supersonic aircraft) according to the embodiment of the present invention.
[Fig. 9] A graph showing a dimensional radius of curvature of the leading edge of the wing (supersonic aircraft)

according to the embodiment of the present invention.

[Fig. 10] A graph showing a non-dimensionalized radius of curvature of the leading edge of the wing (supersonic aircraft) according to the embodiment of the present invention.

[Fig. 11] A diagram for describing cross-flow instability of the wing.

[Fig. 12] A diagram for describing generation of a longitudinal vortex-shaped flow due to the cross-flow instability of the wing and transition from a laminar flow to a turbulent flow.

[Fig. 13] A graph showing a profile of a pressure distribution associated with a cross-flow component of the wing (supersonic aircraft) according to an example not covered by the presently claimed invention but helpful for understanding features thereof.

[Fig. 14] A graph showing a profile of a pressure distribution associated with a cross-flow component of the wing (supersonic aircraft) according to Patent Literature 1.

[Fig. 15] A graph showing a transition point map of transition analysis results in the wing (supersonic aircraft) according to an example not covered by the presently claimed invention but helpful for understanding features thereof.

[Fig. 16] A graph showing a transition point map of transition analysis results in the wing (supersonic aircraft) according to Patent Literature 1.

[Fig. 17] A diagram showing pressure distributions (Cp) on an upper surface of the vicinity of a leading edge of a wing (subsonic aircraft) according to the embodiment of the present invention.

[Fig. 18] A diagram showing pressure distributions (Cp) on an upper surface of the vicinity of a leading edge of a wing (subsonic aircraft) according to Patent Literature 1.

[Fig. 19] A diagram showing a cross-sectional shape of an airfoil (subsonic aircraft) of a wing according to the embodiment of the present invention, which is non-dimensionalized.

[Fig. 20] An enlarged view of the vicinity of the leading edge of the cross-sectional shape shown in Fig. 19.

[Fig. 21] A graph showing a non-dimensional radius of curvature of the vicinity of the leading edge including both of an upper surface and a lower surface of the wing (subsonic aircraft) according to the embodiment of the present invention.

[Fig. 22] A graph showing a dimensional radius of curvature of the leading edge of the wing (subsonic aircraft) according to the embodiment of the present invention.

[Fig. 23] A graph showing a non-dimensionalized radius of curvature of the leading edge of the wing (subsonic aircraft) according to the embodiment of the present invention.

[Fig. 24] A graph showing a profile of a pressure distribution associated with a cross-flow component of the wing (subsonic aircraft) according to an example not covered by the presently claimed invention but helpful for understanding features thereof.

[Fig. 25] A graph showing a profile of a pressure distribution associated with a cross-flow component of the wing (subsonic aircraft) according to Patent Literature 1.

[Fig. 26] A graph showing a transition point map of transition analysis results in the wing (subsonic aircraft) according to an example not covered by the presently claimed invention but helpful for understanding features thereof.

[Fig. 27] A graph showing a transition point map of transition analysis results in the wing (subsonic aircraft) according to Patent Literature 1.

Mode(s) for Carrying Out the Invention

[0018] Hereinafter, an embodiment of the present invention will be described with reference to the drawings.

[0019] Figs. 1 and 2 are diagrams for describing a wing according to the embodiment of the present invention. Fig. 1 shows a top view of the wing as a main wing of an aircraft. Fig. 2 shows a cross-sectional view of the wing. Fig. 1 shows one of two main wings. Fig. 2 shows a vertical cross-sectional view of the wing shown in Fig. 1, which is taken at an arbitrary position in a wingspan direction.

[0020] As shown in Fig. 1, the wing 1 according to the embodiment of the present invention is typically used as a main wing of an aircraft 100. The reference sign 101 designates a fuselage of the aircraft 100. The aircraft 100 may be a supersonic aircraft or may be a subsonic aircraft. Moreover, the wing 1 is a swept-back wing having a swept-back angle A.

[0021] In Figs. 1 and 2, the x-axis indicates an axis in a wing chord direction, the y-axis indicates an axis in a wingspan (span) direction, and the z-axis indicates an axis in a wing thickness direction.

[0022] The origin on the x-axis is a leading edge 11. The +direction of the x-axis is a direction from the leading edge 11 to a trailing edge 12. The origin on the y-axis is an aircraft axis 14 of the aircraft 100. The +direction of the y-axis is a direction from the aircraft axis 14 to a wing tip 15. The origin of the z-axis is a wing chord line 16 (Fig. 2). The +direction of the z-axis is a direction upward from the wing 1.

[0023] Moreover, in order to non-dimensionalize a position in the wing chord direction (x-direction), a position in the wingspan direction (y-direction), and a position in the wing thickness direction (z-direction) in the wing 1, those positions are each divided by a local wing chord length c of the wing 1 or a semi-span length s of the wing 1. The non-dimensionalized

position (x/c) in the wing chord direction (x-direction), the non-dimensionalized position (y/s) in the wingspan direction (y-direction), and the non-dimensionalized position (z/c) in the wing thickness direction (z-direction) are defined.

In Case of Supersonic Aircraft

[0024] Hereinafter, an embodiment in a case where the present invention is applied to a supersonic aircraft will be described.

Pressure Distribution (Cp)

[0025] Fig. 3 is a diagram showing pressure distributions (Cp) on an upper surface of the vicinity of the leading edge 11 of the wing 1, according to the presently claimed invention.

[0026] Here, Cp_ys10 represents a pressure distribution (Cp) based on the non-dimensionalized position in the wing chord direction (x-direction) in a case where the non-dimensionalized position (y/s) in the wingspan direction (y-direction) is a position of 10%. The same applies to the following symbols, and Cp_ys20 represents a pressure distribution (Cp) based on the non-dimensionalized position in the wing chord direction (x-direction) in a case where the non-dimensionalized position (y/s) in the wingspan direction (y-direction) is a position of 20%.

[0027] Fig. 4 shows similar pressure distributions (Cp) according to Patent Literature 1 as a reference example. Those pressure distributions (Cp) have substantially the same gradients at all positions in the wingspan (span) direction. The wing 1 according to the present invention is thus clearly different from the pressure distributions according to Patent Literature 1 in this point.

[0028] The pressure distribution (Cp) on the upper surface of the vicinity of the leading edge 11 of the wing 1, which are shown in Fig. 3, can be typically expressed by the following function.

[Expression 1]

$$Cp(\xi,\eta) = \sum_{i=0}^{n} A_i(\eta) f_i(\xi,\eta)$$

$$\xi \equiv x/c,$$

$$\eta \equiv y/s$$

$$f_0(\xi,\eta) \equiv 1,$$

$$f_i(\xi,\eta) \equiv \exp[\, B_i(\eta)\xi^{P_i}\,] - 1, \qquad i = 1,\cdots,n-1$$

$$f_n(\xi,\eta) \equiv \xi^{P_n}$$

(Expression 1)

where n = 5 in a case of the supersonic aircraft and n = 7 in a case of the subsonic aircraft.

[0029] In that function, the rising gradients of the vicinity of the leading edge 11 in the wingspan (span) direction can be typically determined in accordance with the following relational expression.

[Expression 2]

$$B_2(\eta) = \left(\Lambda_{LE}(\eta) \sum_{i=0}^{2} \alpha_i \eta^i \right) \times \textit{fudge factor}$$

where $\eta \equiv y/s$

$\Lambda_{LE} \equiv$ *Swept-back Angle at* η *station* [rad]

fudge factor $\equiv$ *Fine adjustment factor for adjusting Re number effect and the like. (used in range of [0, 1] considering case of size of actual aircraft with highly swept-back wing, high-Reynolds number as 1)*

$\alpha_0 = -105000$

$\alpha_1 = 198000$

$\alpha_2 = -95000$

(Expression 2)

Airfoil

[0030] Regarding the airfoil of the wing 1, according to the presently claimed invention the dimensionalized radius of curvature of the leading edge 11 typically decreases from the wing root 17 to the wing tip 15.

[0031] Such a shape can be obtained by using the CFD-based inverse problem design process of determining the cross-sectional wing shape on the basis of the above-mentioned pressure distributions (Cp) of the wing 1, which has been described above. The CFD-based inverse problem design process typically includes: a process of setting an initial shape of a cross-sectional wing shape; a CFD analysis process of determining pressure distribution of a flow-field in the vicinity of the cross-sectional wing shape obtained; a transition analysis process of estimating a boundary layer transition position on a wing surface; a process of setting target pressure distributions for wing upper and lower surfaces based on the pressure distribution; and a CFD-based inverse problem design process including the CFD analysis process and a shape correction process "correcting the cross-sectional wing shape such that the pressure distribution obtained from the CFD analysis process converges on the target pressure distribution." The CFD-based inverse problem design process is described in detail in Patent Literature 1 (Japanese Patent No. 5747343). A more specific design example will be described with reference to Fig. 5. Fig. 5 shows the leading edge of the wing 1 in an enlarged state. Here, a design is made by determining parameters as follows at positions A_0 to B_2 shown in Fig. 5.

A_0: pressure at leading edge (use Cp distribution for initial shape)
A_1: rising pressure value at each spanwise station of leading edge portion
A_2: Set to value close to average value of minimum pressure level at each spanwise station
A_3 to An: Adjust Cp distribution
B_1: Make negative values with larger absolute values
B_2: Make negative values with absolute values gradually smaller at each spanwise station from wing root to the wing tip

[0032] Important parameters of the vicinity of the leading edge of the wing 1 can be thus determined. The airfoil can be determined. The wing 1 having reduced friction drag can be easily designed.

[0033] With this, the wing 1 is configured such that the surface pressure of the vicinity of the leading edge 11 of the surface in the fluid increases from the wing root 17 to the wing tip 15. The airfoil of the wing 1 as an aspect thereof is typically configured such that the dimensionalized radius of curvature of the leading edge 11 decreases from the wing root 17 to the wing tip 15 while the non-dimensionalized radius of curvature of the leading edge 11 increases from the wing root 17 to the wing tip 15.

[0034] Figs. 6 and 7 show a shape example of the airfoil of such a wing , according to the presently claimed invention. Fig. 6 shows non-dimensionalized cross-sectional shape of the wing 1. Fig. 7 shows an enlarged view of the vicinity of the leading edge 11 of Fig. 6.

[0035] Figs. 8, 9, and 10 each show a radius of curvature of the leading edge of the wing 1 shown in Figs. 6 and 7, according to the presently claimed invention. Fig. 8 shows a non-dimensional radius of curvature of the vicinity of the leading edge 11 including both of an upper surface and a lower surface (x/c+ is the upper surface and - is the lower surface). Fig. 9 shows a dimensional radius of curvature (m) of the leading edge 11. Fig. 10 shows a radius of curvature non-dimensionalized with the local wing chord length of the leading edge 11. Moreover, in either case, the position of the wingspan (span) direction (y-direction) is non-dimensionalized (y/s). It should be noted that in Figs. 9 and 10, the open circle (◦) represents the radius of curvature of the leading edge of the wing 1 according to the present invention and the filled circle (•) represents the radius of curvature of the leading edge of the wing according to Patent Literature 1 as an reference example.

[0036] As shown in Fig. 9, as the dimensional radius of curvature of the leading edge of the wing 1 according to the present invention is compared to that of Patent Literature 1, the radius of curvature decreases from the wing root to the wing tip in the both cases at positions in the wingspan (span) direction which excludes the vicinity of the wing root (range of y/s = approximately 0 to 0.02). However, as can be seen from Fig. 10, as the non-dimensional radius of curvature of the leading edge of the wing 1 according to the present invention is compared to that of Patent Literature 1, the non-dimensional radius of curvature of the leading edge of Patent Literature 1 decreases from the wing root to the wing tip while the non-dimensional radius of curvature of the leading edge 11 of the wing 1 according to the present invention increases from the wing root 17 to the wing tip 15. The wing 1 according to the present invention is thus clearly different from the airfoil according to Patent Literature 1 in this point.

Actions and Effects

[0037] The above-mentioned wing 1 is configured such that a cross-flow component of an external streamline of the surface of the wing 1 is thus reduced in the vicinity of the leading edge 11. The boundary layer transition is not easily induced in the vicinity of the leading edge 11.

[0038] Drag which acts on an object moving through a fluid is classified into friction drag, induced drag, and wave drag (see Fig. 8 of Patent Literature 1).

[0039] The friction drag depends on state of a flow in the boundary layer. In a case of a laminar boundary layer, the friction drag is small in comparison with a case of a turbulent boundary layer (boundary layer stability theory: see Fig. 9 of Patent Literature 1).

[0040] Considering an aircraft as an example, maintaining a flow around an aircraft body during a flight as a laminar flow contributes to reduction of friction drag (see the laminar boundary layer and the turbulent boundary layer in Fig. 2).

[0041] Although laminarization of an aircraft body such as a wing is thus desirable, the flow around the aircraft body transitions from the laminar flow to the turbulent flow, depending on a flight condition (see Fig. 8 of Patent Literature 1).

[0042] Aerodynamic phenomena which can cause the boundary laminar flow to transition from the laminar flow to the turbulent flow are classified into two phenomena. One is Tollmien-Schichting (T-S) instability and the other is cross-flow (C-F) instability (see Fig. 10 of Patent Literature 1).

[0043] The transition due to the C-F instability is a dominant factor which can cause transition of an object shape (wing) having a large swept-back angle.

[0044] When a cross-flow velocity component is larger with respect to a direction of a boundary layer outer edge flow, the C-F instability remarkably develops, which causes transition of the boundary layer from the laminar flow to the turbulent flow.

[0045] That is, as shown in Fig. 11, in a case where the wing 1 has a swept-back angle A, a leading-edge parallel component Si of a main stream is not affected by influence of a pressure gradient caused by the wing cross-section while a leading-edge orthogonal component S_2 is affected by the influence of the pressure gradient caused by the wing cross-section. Therefore, an external streamline (stream line at a boundary layer upper end) u_e bends (reference sign S_3). A velocity component perpendicular to the stream line, that is, a cross-flow component w is generated due to bend of the external streamline u_e. The cross-flow component w has an inflection point i_p. When the velocity component has the inflection point, the flow is unstable in accordance with Rayleigh's inflection point theorem. That instability will be referred to as cross-flow instability. Then, as shown in Fig. 12, a longitudinal vortex-shaped flow v approximately parallel to the external streamline u_e due to that cross-flow instability is generated, and it transitions from the laminar flow to the turbulent flow.

[0046] Fig. 13 is a graph showing a profile of a pressure distribution associated with a cross-flow component of the wing 1 according to an example not covered by the presently claimed invention but helpful for understanding features thereof. Fig. 14 shows a profile of a pressure distribution associated with a cross-flow component of the wing according to Patent Literature 1 as an reference example. The both are the profile of the pressure distribution at a position of (y/s) = 0.3 in the wingspan direction. In those figures, δ of y/δ of the vertical axis is a thickness of the boundary layer and is a distance between the boundary layer, which is shown as a line dividing a flow above the wing cross-section shown in Fig. 2 into upper and lower parts, and the wing surface.

[0047] As can be seen from those figures, in the wing 1 according to an example not covered by the presently claimed invention but helpful for understanding features thereof, the ratio of the cross-flow component w to the external streamline u_e (w/u_e) is smaller in the vicinity of the leading edge 11 of the wing 1 as compared to the wing according to Patent Literature 1 and the cross-flow component w is suppressed.

[0048] Fig. 15 is a graph showing a transition point map of transition analysis results in the wing 1 according to an example not covered by the presently claimed invention but helpful for understanding features thereof. Fig. 16 shows a transition point map of transition analysis results in the wing according to Patent Literature 1 as a reference example. Those graphs show a dimensional wing as viewed from the upper surface. In those figures, N is an amplification factor of unstable waves (wavy fluctuations due to the cross-flow instability) which introduce the transition process of the boundary layer from the laminar flow to the turbulent flow, and a specific value of N, for example, 12, 13, or 14 is a transition position depending on velocity of flow, test conditions, surface roughness, and the like.

[0049] As can be seen from those figures, in the wing 1 according to an example not covered by the presently claimed invention but helpful for understanding features thereof, the transition position is moved to a downstream side of the wing and a laminar flow region is wider as compared to the wing according to Patent Literature 1.

[0050] In Case of Subsonic Aircraft

[0051] The present invention can be applied not only to the supersonic aircraft but also to the subsonic aircraft.

Pressure Distribution (Cp)

[0052] Fig. 17 is a diagram showing pressure distributions (Cp) in an upper surface of the vicinity of a leading edge 11 of a wing 1 of a subsonic aircraft, according to the presently claimed invention.

[0053] In those pressure distributions in the vicinity of the leading edge 11, the rising gradients are made systematically gentler, meaning it decreases, from Cp_ys10 to Cp_ys100, that is, from the wing root 17 to the wing tip 15 of the upper surface of the wing 1.

[0054] Fig. 18 shows similar pressure distributions (Cp) according to Patent Literature 1 as an reference example. Those pressure distributions (Cp) have substantially the same gradients at all positions in the wingspan (span) direction. The wing 1 of the subsonic aircraft according to the present invention is thus clearly different from the pressure distributions (Cp) according to Patent Literature 1 in this point.

[0055] The pressure distribution (Cp) on the upper surface of the vicinity of the leading edge 11 of the wing 1, which are shown in Fig. 17 can be typically expressed as n = 7 in the function shown in Expression 1 above. Moreover, the rising gradients of the vicinity of the leading edge 11 in the wingspan (span) direction in that function can be typically determined in accordance with the relational expression shown in Expression 2.

Airfoil

[0056] As in the supersonic aircraft, the airfoil of the wing 1 of the subsonic aircraft is typically configured such that the dimensionalized radius of curvature of the leading edge 11 decreases from the wing root 17 to the wing tip 15.

[0057] Figs. 19 and 20 show a shape of the airfoil of such a wing , according to the presently claimed invention. Fig. 19 shows a non-dimensionalized cross-sectional shape of the wing 1. Fig. 20 shows an enlarged view of the vicinity of the leading edge 11 of Fig. 19.

[0058] Figs. 21, 22, and 23 each show a radius of curvature of the leading edge of the wing 1 shown in Figs. 19 and 20, according to the presently claimed invention. Fig. 21 shows a non-dimensional radius of curvature of the vicinity of the leading edge 11 including both of an upper surface and a lower surface (x/c+ is the upper surface and - is the lower surface). Fig. 22 shows a dimensional radius of curvature (m) of the leading edge 11. Fig. 23 shows a non-dimensionalized radius of curvature of the leading edge 11. It should be noted that in Figs. 22 and 23, the open circle (◦) represents the radius of curvature of the leading edge of the wing 1 according to the present invention and the filled circle (•) represents the radius of curvature of the leading edge of the wing according to Patent Literature 1 as an reference example.

[0059] As shown in Fig. 22, as the dimensional radius of curvature of the leading edge of the wing 1 according to the present invention is compared to that of Patent Literature 1, the radius of curvature decreases from the wing root to the wing tip in the both cases. However, as can be seen shown in Fig. 23, as the non-dimensional radius of curvature of the leading edge of the wing 1 according to the present invention is compared to that of Patent Literature 1, the non-dimensional radius of curvature of the leading edge of Patent Literature 1 decreases from the wing root to the wing tip. The wing 1 of the subsonic aircraft according to the present invention is thus clearly different from the airfoil according to Patent Literature 1 in this point.

Actions and Effects

[0060] The wing 1 of the subsonic aircraft has actions and effects similar to those of the supersonic aircraft described above. That is, the wing 1 of the subsonic aircraft according to the present invention is configured such that the pressure distribution (Cp) on the upper surface of the vicinity of the leading edge 11 increases from the wing root 17 to the wing tip 15 as in the supersonic aircraft. Therefore, the cross-flow component w can be reduced and the transition from the laminar flow to the turbulent flow due to the C-F instability can be suppressed. With this, the friction drag caused by the C-F instability can be reduced.

[0061] Fig. 24 is a graph showing a profile of a pressure distribution associated with a cross-flow component of the wing 1 of the subsonic aircraft according to an example not covered by the presently claimed invention but helpful for understanding features thereof. Fig. 25 shows a profile of a pressure distribution associated with a cross-flow component of the wing of the subsonic aircraft according to Patent Literature 1 as a reference example. The both are the profile of the pressure distribution at a position of (y/s) = 0.3 in the wingspan direction.

[0062] As can be seen from those figures, in the wing 1 of the subsonic aircraft according to the present invention, the ratio of the cross-flow component w to the external streamline u_e (w/u_e) is smaller in the vicinity of the leading edge 11 of the wing 1 and the cross-flow component w is suppressed as compared to the wing according to Patent Literature 1.

[0063] Fig. 26 is a graph showing a transition point map of transition analysis results in the wing 1 of the subsonic aircraft according to an example not covered by the presently claimed invention but helpful for understanding features thereof. Fig. 27 shows a transition point map of transition analysis results in the wing according to Patent Literature 1 as a reference example.

[0064] As can be seen from those figures, in the wing 1 according to the present invention, the transition point is moved to the downstream side of the wing and the laminar flow region is wider as compared to the wing according to Patent Literature 1.

Conclusion

[0065] In the wing 1 according to the above-mentioned embodiment, the cross-flow component can be thus reduced.

The transition from the laminar flow to the turbulent flow can be suppressed. With this, the friction drag caused by the cross-flow instability can be reduced.

[0066] Moreover, with this wing 1, an ideal pressure distribution suitable for natural laminarization is determined by grasping a relationship between a pressure distribution and transition by using a transition point prediction method, and its shape is also determined. Therefore, it is easy to make a design.

[0067] Furthermore, the leading-edge shape is not sharper toward the wing tip 15, and it is also easy to manufacture it.

[0068] It should be noted that the present invention is not limited to the above-mentioned embodiment, various modifications and applications can be made, the scope of protection being defined by the appended claims.

[0069] For example, by applying the present invention to a fin stabilizer to be used for a watercraft and the like, it can also serve to reduce large drag on the watercraft body at sea owing to laminarization of the stabilizer.

Reference Signs List

[0070]

1	wing
11	leading edge
15	wing tip
17	wing root
100	aircraft
A	swept-back angle

Claims

1. A wing (1) having a swept-back angle (A) when attached to an aircraft (100), **characterized in that** for any given value x/c within a range of 0% to 5% from a leading edge (11), a gradient of a pressure coefficient (Cp) on the upper surface of the wing (1) decreases from a wing root (17) to a wing tip (15).

2. The wing (1) according to the previous claim, which is configured such that
a radius of curvature of the leading edge (11) shows a first tendency to decrease from the wing root (17) to the wing tip (15).

3. An aircraft (100) comprising the wing (1) according to any one of the previous claims.

Patentansprüche

1. Flügel (1), der, wenn er an einem Flugzeug (100) befestigt ist, einen Rückpfeilungswinkel (A) aufweist,
dadurch gekennzeichnet, dass
für einen beliebigen vorgegebenen Wert x/c innerhalb eines Bereichs von 0% bis 5% von einer Vorderkante (11) ein Gradient eines Druckkoeffizienten (Cp) auf der oberen Fläche der Flügel (1) von einer Flügelwurzel (17) zu einer Flügelspitze (15) abnimmt.

2. Flügel (1) nach dem vorhergehenden Anspruch, der derart konfiguriert ist, dass ein Krümmungsradius der Vorderkante (11) eine erste Tendenz zeigt, von der Flügelwurzel (17) zur Flügelspitze (15) abzunehmen.

3. Flugzeug (100) mit dem Flügel (1) nach einem der vorhergehenden Ansprüche.

Revendications

1. Aile (1) ayant un angle de repli vers l'arrière (A) lorsqu'elle est fixée à un aéronef (100), **caractérisée en ce que** pour n'importe quelle valeur de x/c donnée à l'intérieur d'une plage de 0 % à 5 % à partir d'un bord d'attaque (11), un gradient d'un coefficient de pression (Cp) sur la surface supérieure de l'aile (1) diminue depuis une emplanture de l'aile (17) jusqu'à un saumon de l'aile (15).

2. Aile (1) selon la revendication précédente, qui est conçue de telle sorte que

un rayon de courbure du bord d'attaque (11) présente une première tendance à diminuer depuis l'emplanture de l'aile (17) jusqu'au saumon de l'aile (15).

3. Aéronef (100) comprenant l'aile (1) selon l'une quelconque des revendications précédentes.

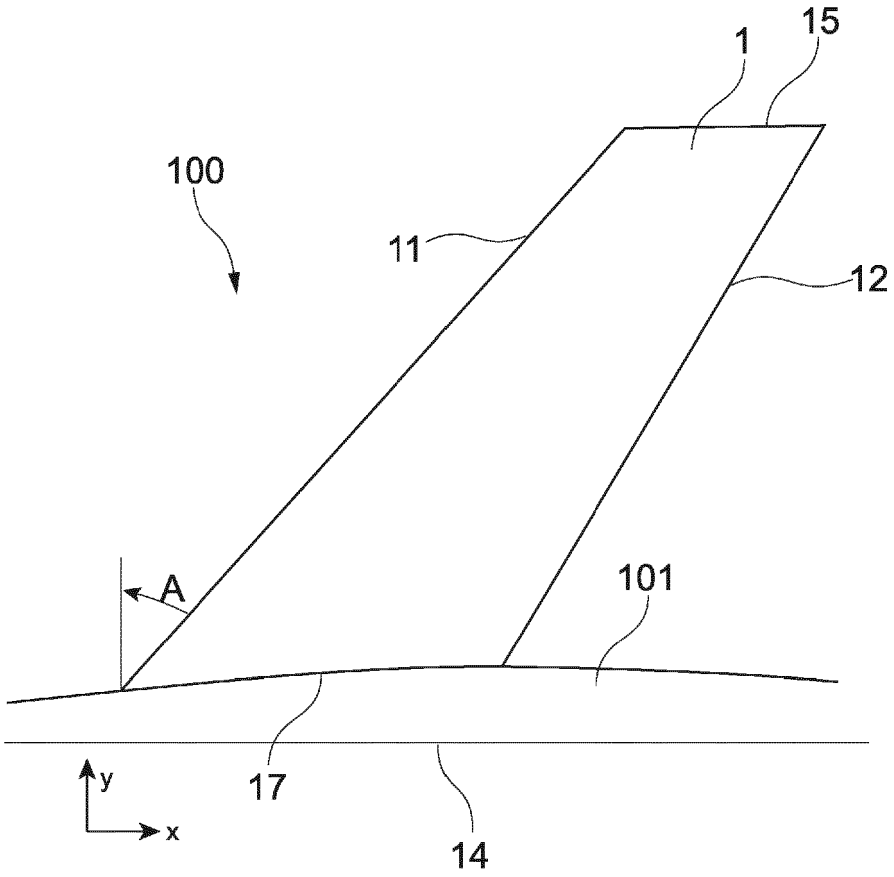

FIG.1

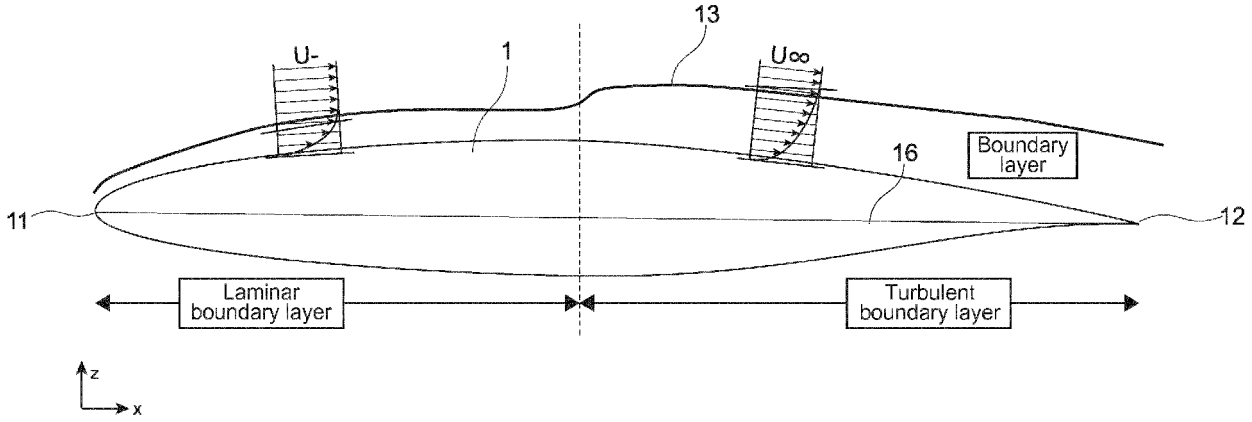
13
U-
1
U∞
16
Boundary layer
11
12
Laminar boundary layer
Turbulent boundary layer
z
x

FIG.2

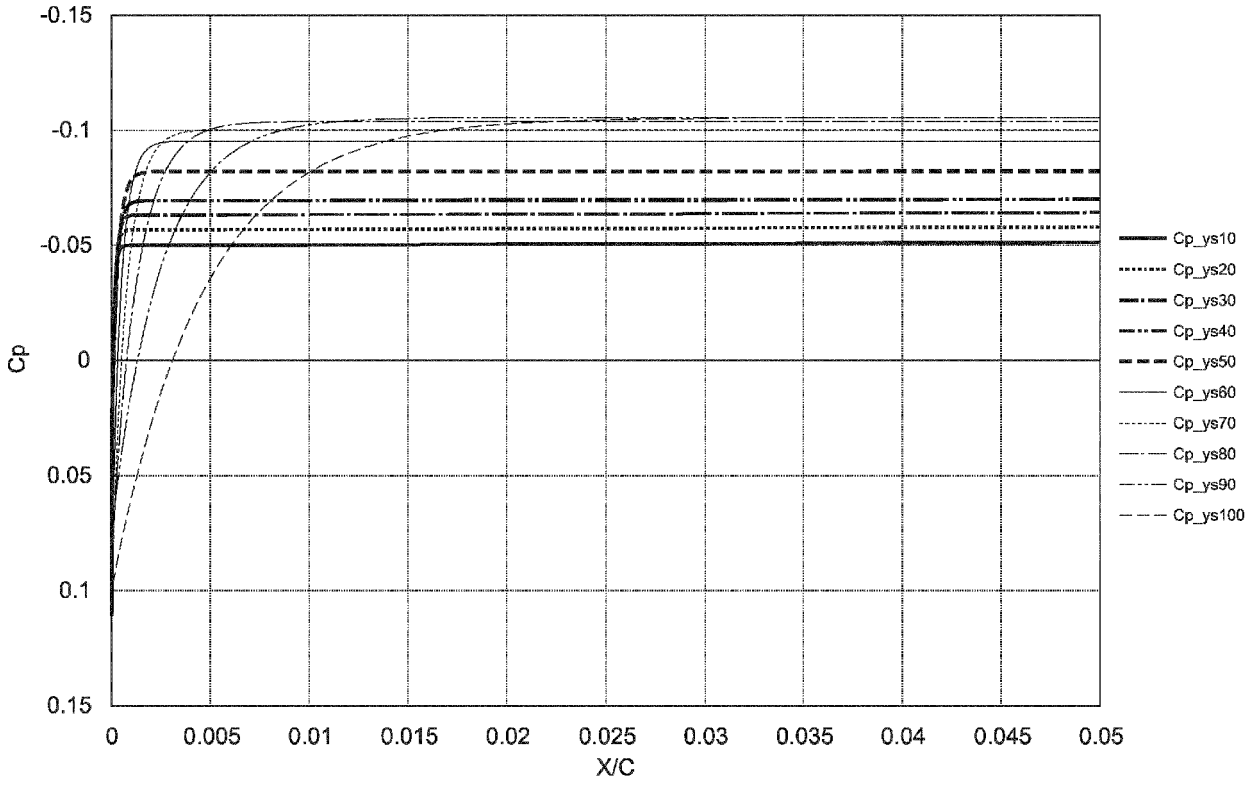
-0.15
-0.1
-0.05
0
0.05
0.1
0.15
Cp
0
0.005
0.01
0.015
0.02
0.025
0.03
0.035
0.04
0.045
0.05
X/C
Cp_ys10
Cp_ys20
Cp_ys30
Cp_ys40
Cp_ys50
Cp_ys60
Cp_ys70
Cp_ys80
Cp_ys90
Cp_ys100

FIG.3

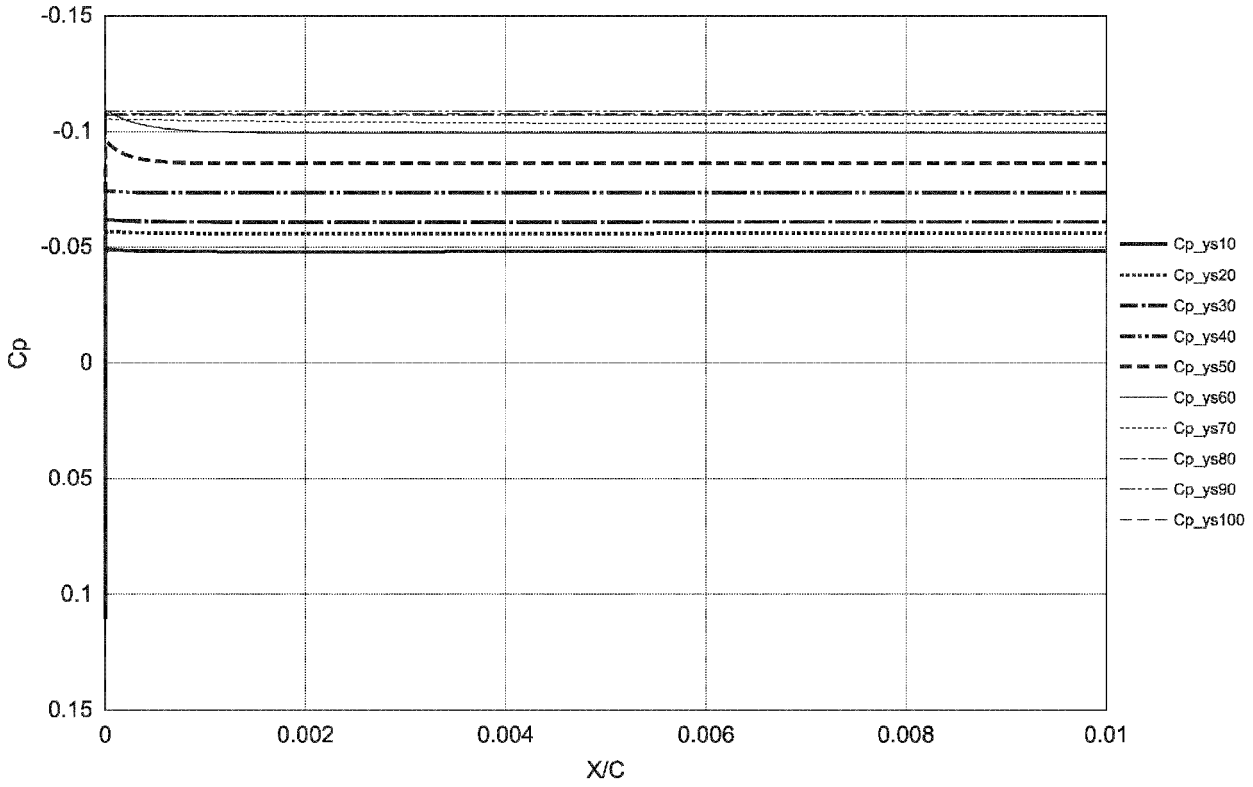
-0.15
-0.1
-0.05
0
0.05
0.1
0.15
Cp
0
0.002
0.004
0.006
0.008
0.01
X/C
Cp_ys10
Cp_ys20
Cp_ys30
Cp_ys40
Cp_ys50
Cp_ys60
Cp_ys70
Cp_ys80
Cp_ys90
Cp_ys100

FIG.4

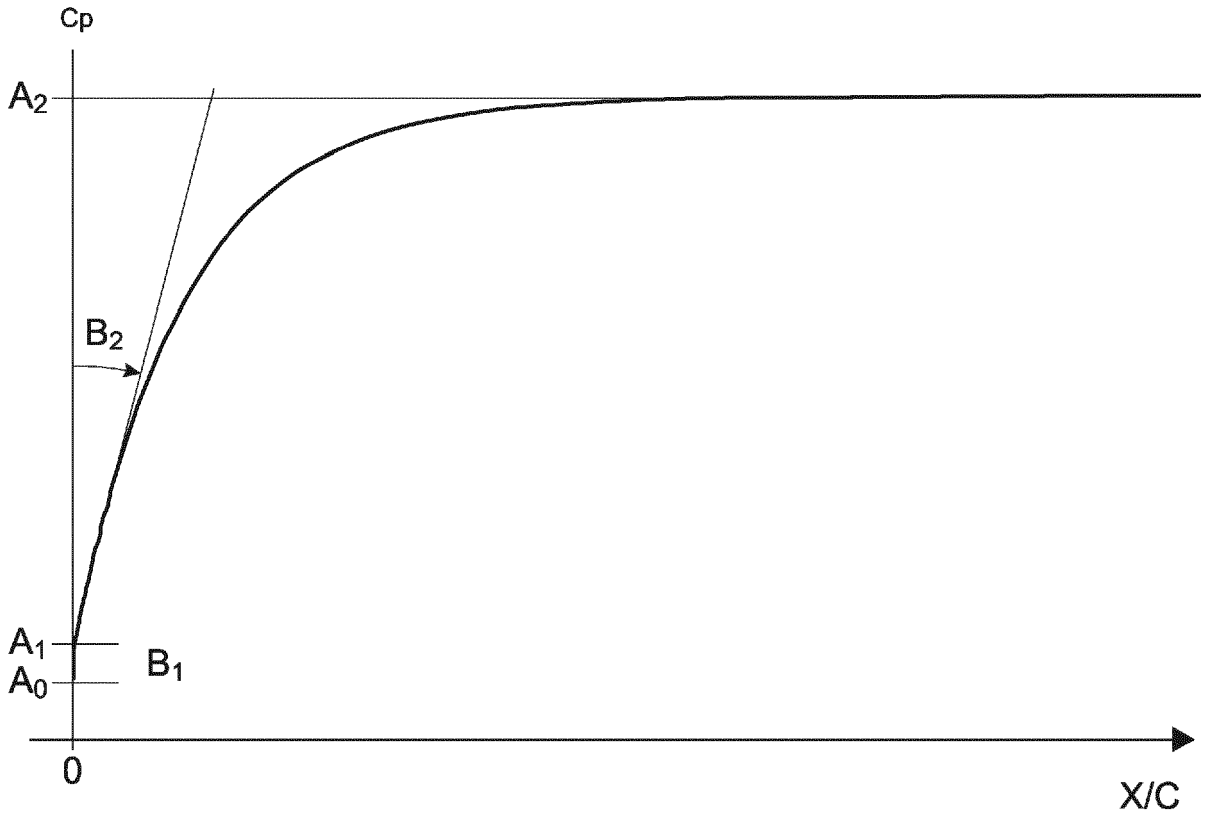

FIG.5

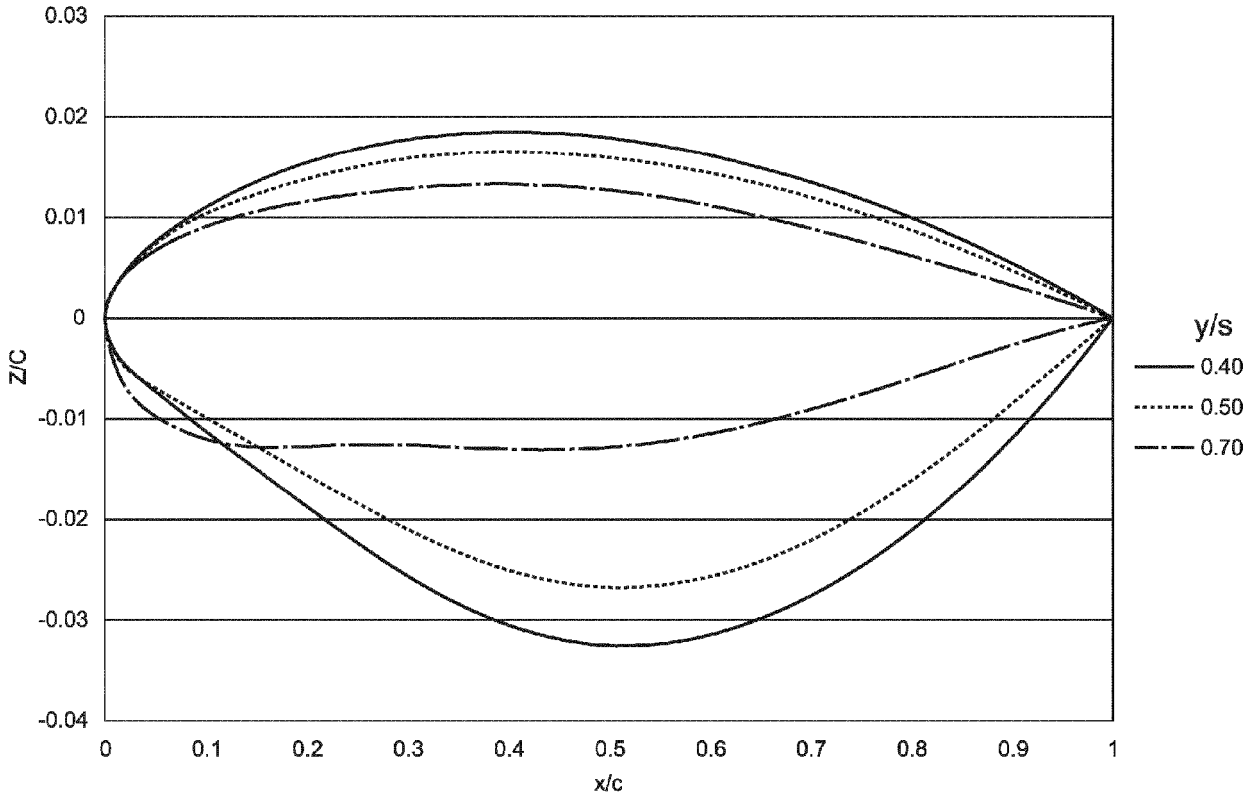
0.03
0.02
0.01
0
-0.01
-0.02
-0.03
-0.04
Z/C
0
0.1
0.2
0.3
0.4
0.5
0.6
0.7
0.8
0.9
1
x/c
y/s
0.40
0.50
0.70

FIG.6

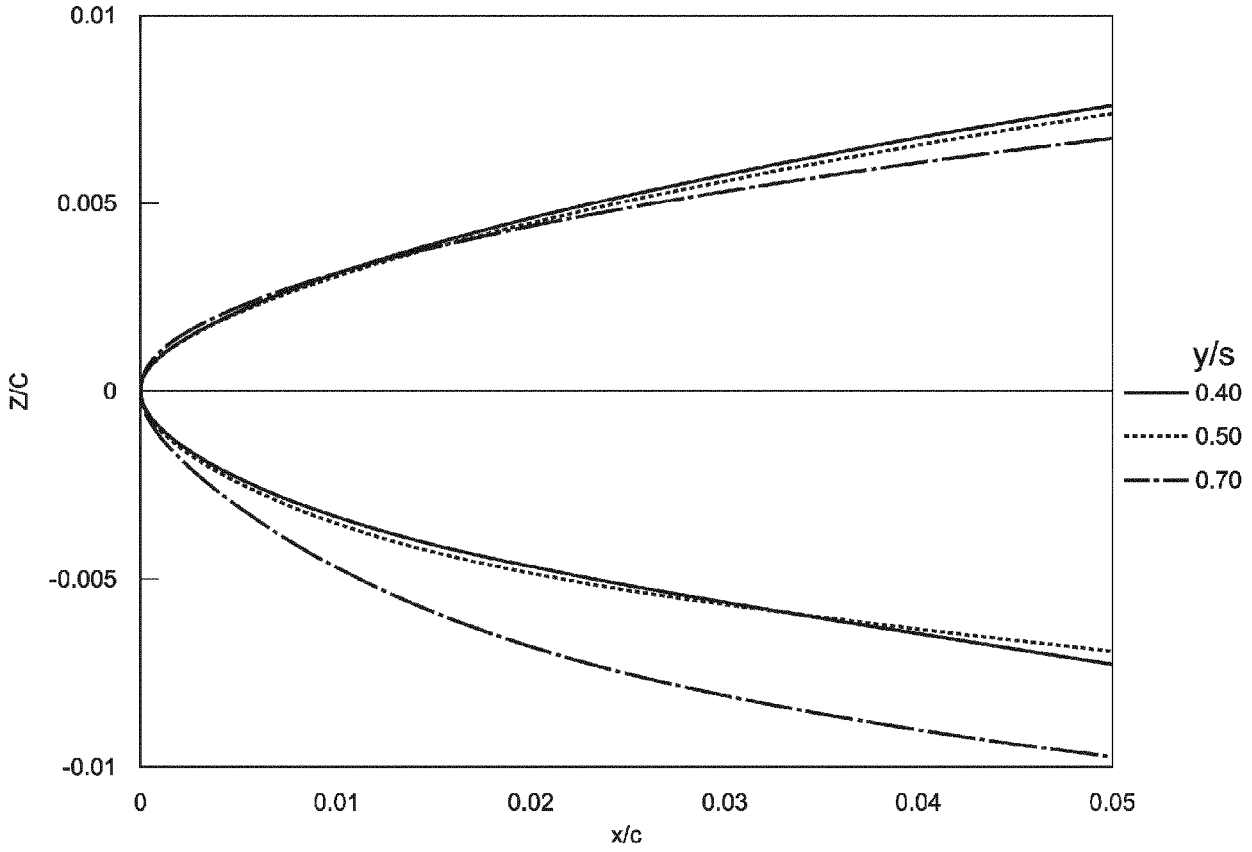

FIG.7

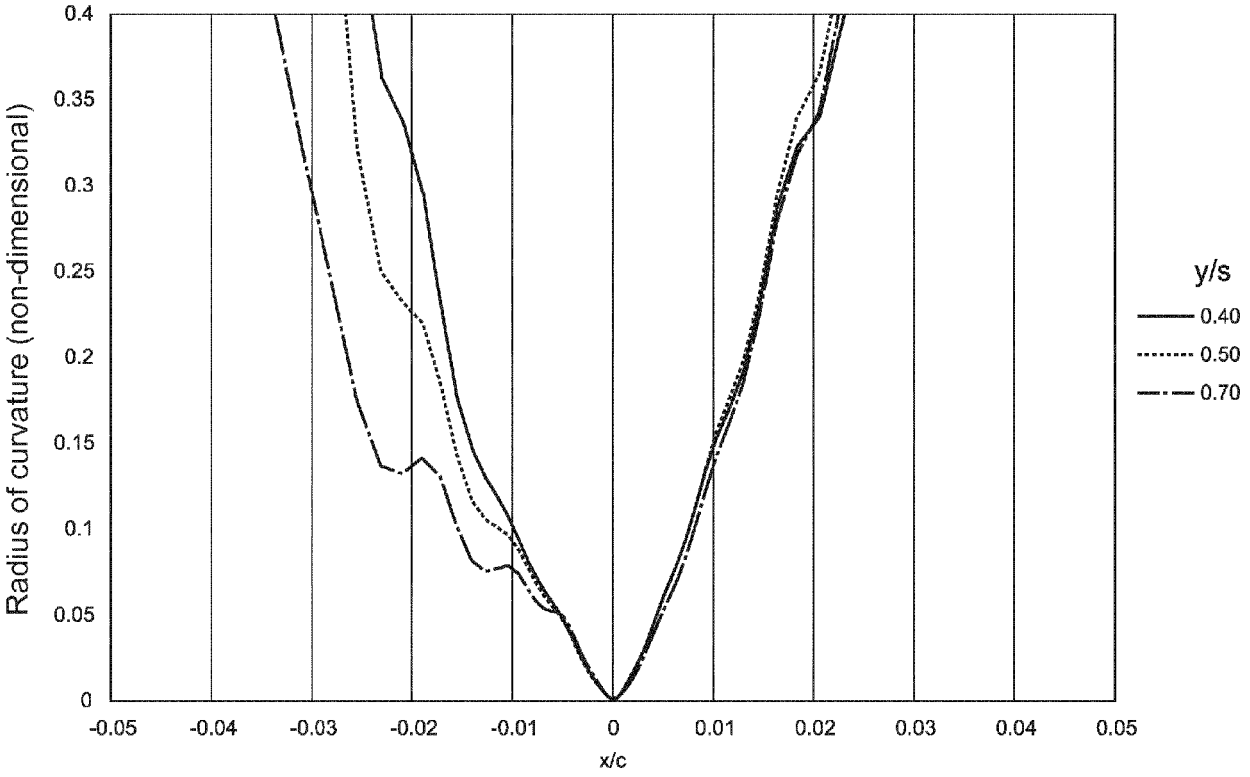
Radius of curvature (non-dimensional)
0.4
0.35
0.3
0.25
0.2
0.15
0.1
0.05
0
-0.05
-0.04
-0.03
-0.02
-0.01
0
0.01
0.02
0.03
0.04
0.05
x/c
y/s
0.40
0.50
0.70

FIG.8

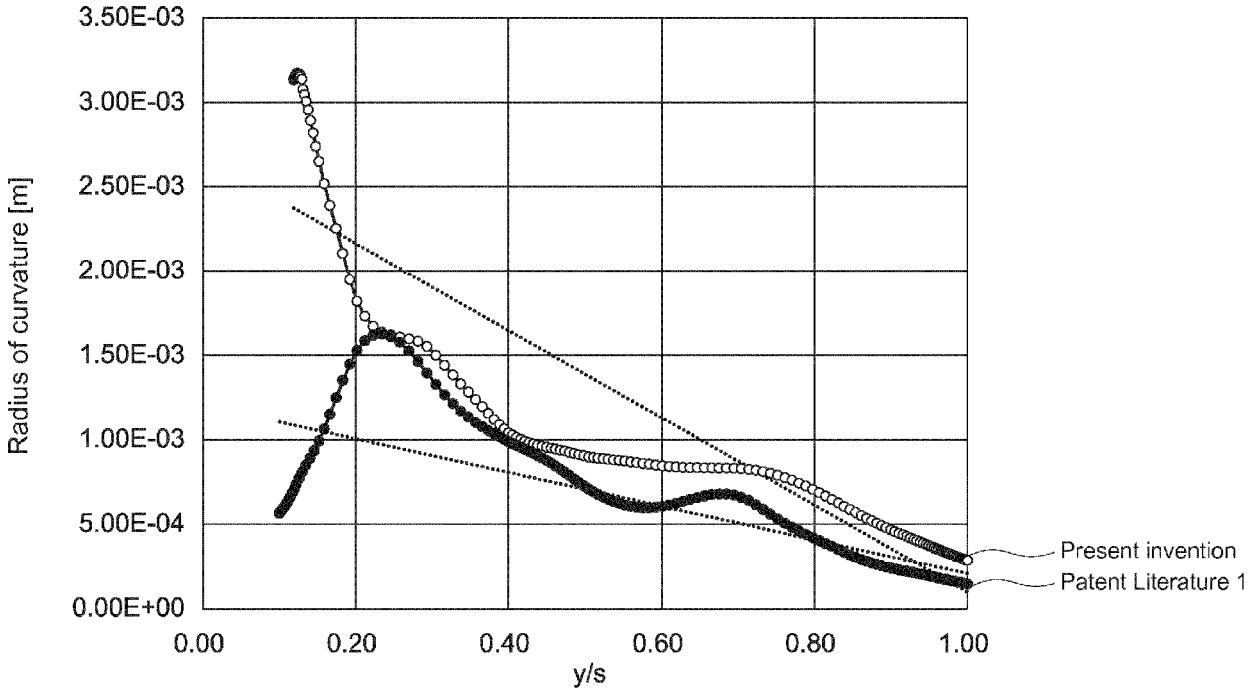
3.50E-03
3.00E-03
2.50E-03
2.00E-03
1.50E-03
1.00E-03
5.00E-04
0.00E+00
Radius of curvature [m]
0.00
0.20
0.40
0.60
0.80
1.00
y/s
Present invention
Patent Literature 1

FIG.9

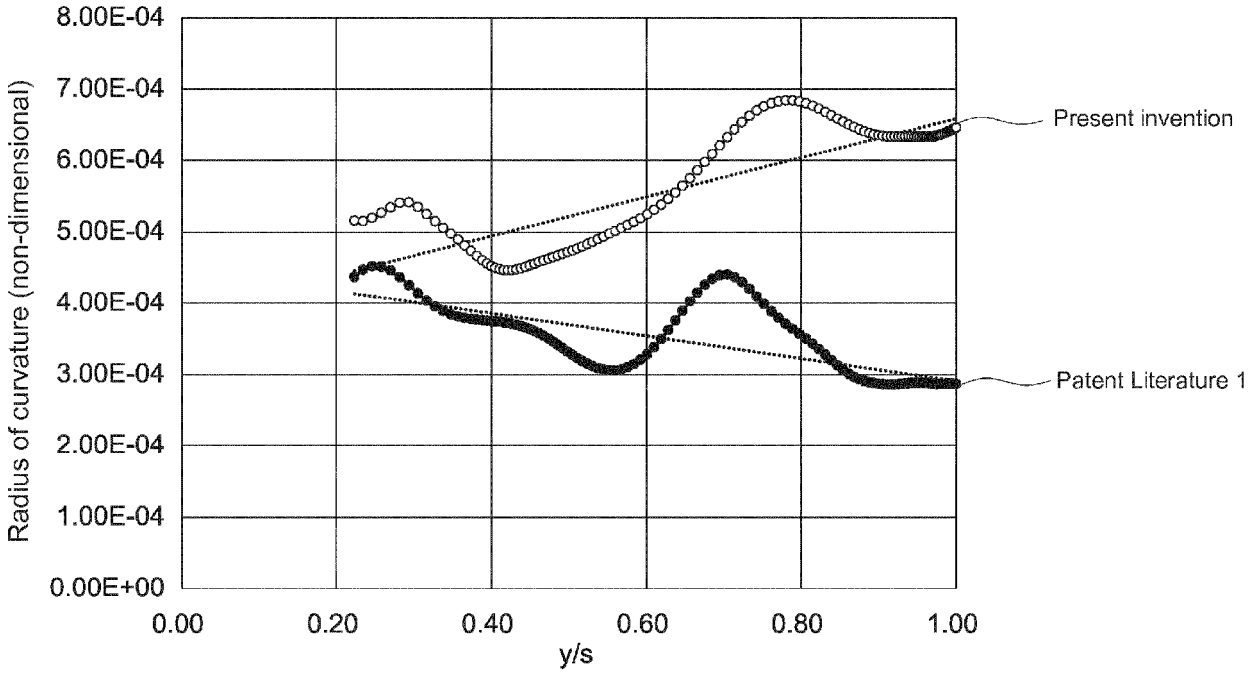
8.00E-04
7.00E-04
6.00E-04
5.00E-04
4.00E-04
3.00E-04
2.00E-04
1.00E-04
0.00E+00
Radius of curvature (non-dimensional)
0.00
0.20
0.40
0.60
0.80
1.00
y/s
Present invention
Patent Literature 1

FIG.10

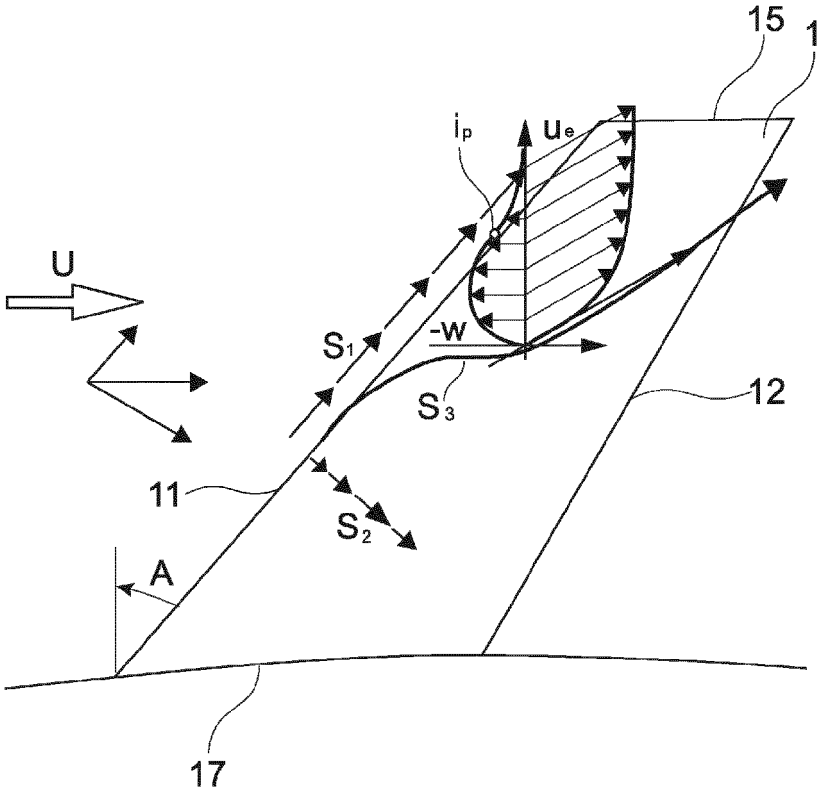

FIG.11

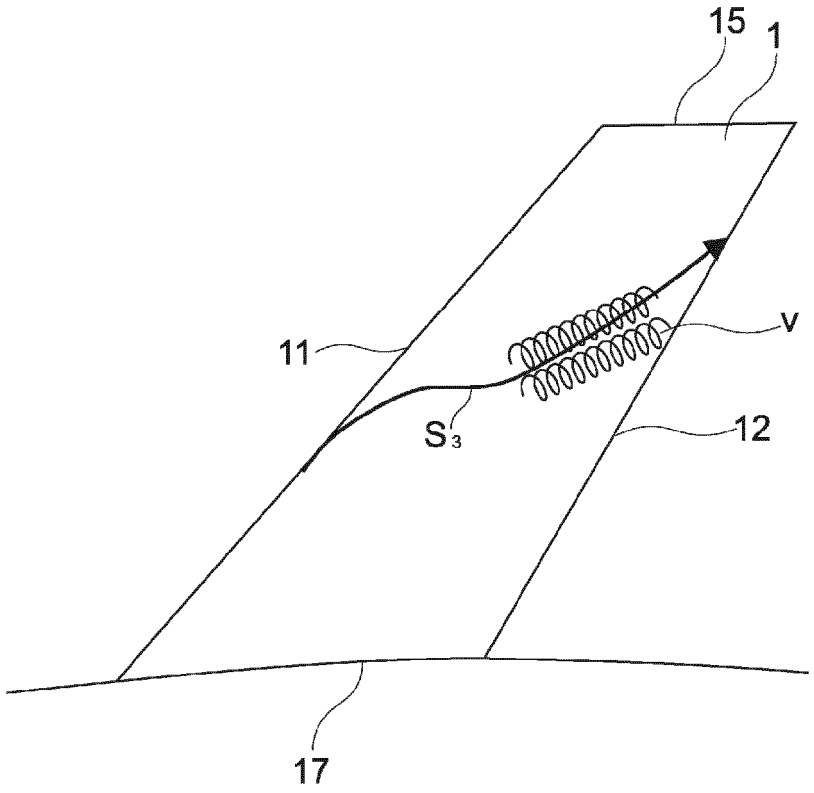

FIG.12

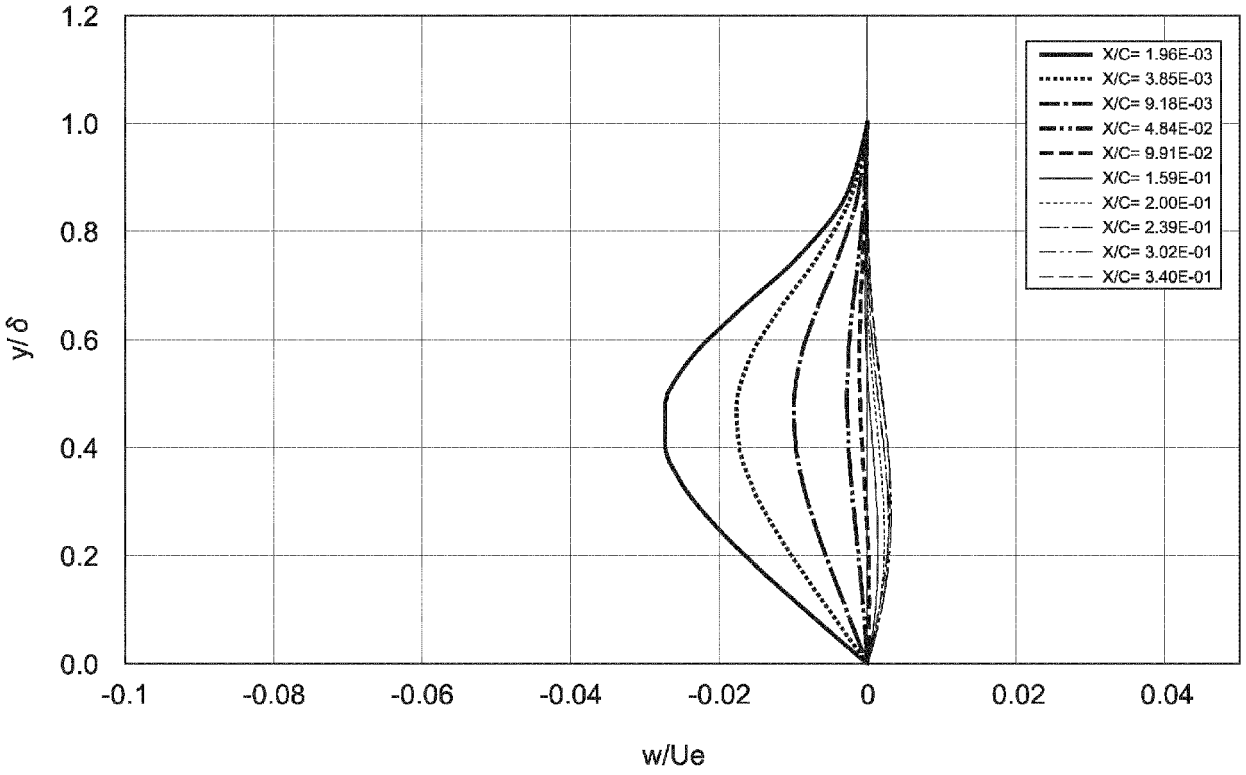
1.2
1.0
0.8
0.6
0.4
0.2
0.0
y/δ
-0.1
-0.08
-0.06
-0.04
-0.02
0
0.02
0.04
w/Ue
X/C= 1.96E-03
X/C= 3.85E-03
X/C= 9.18E-03
X/C= 4.84E-02
X/C= 9.91E-02
X/C= 1.59E-01
X/C= 2.00E-01
X/C= 2.39E-01
X/C= 3.02E-01
X/C= 3.40E-01

FIG.13

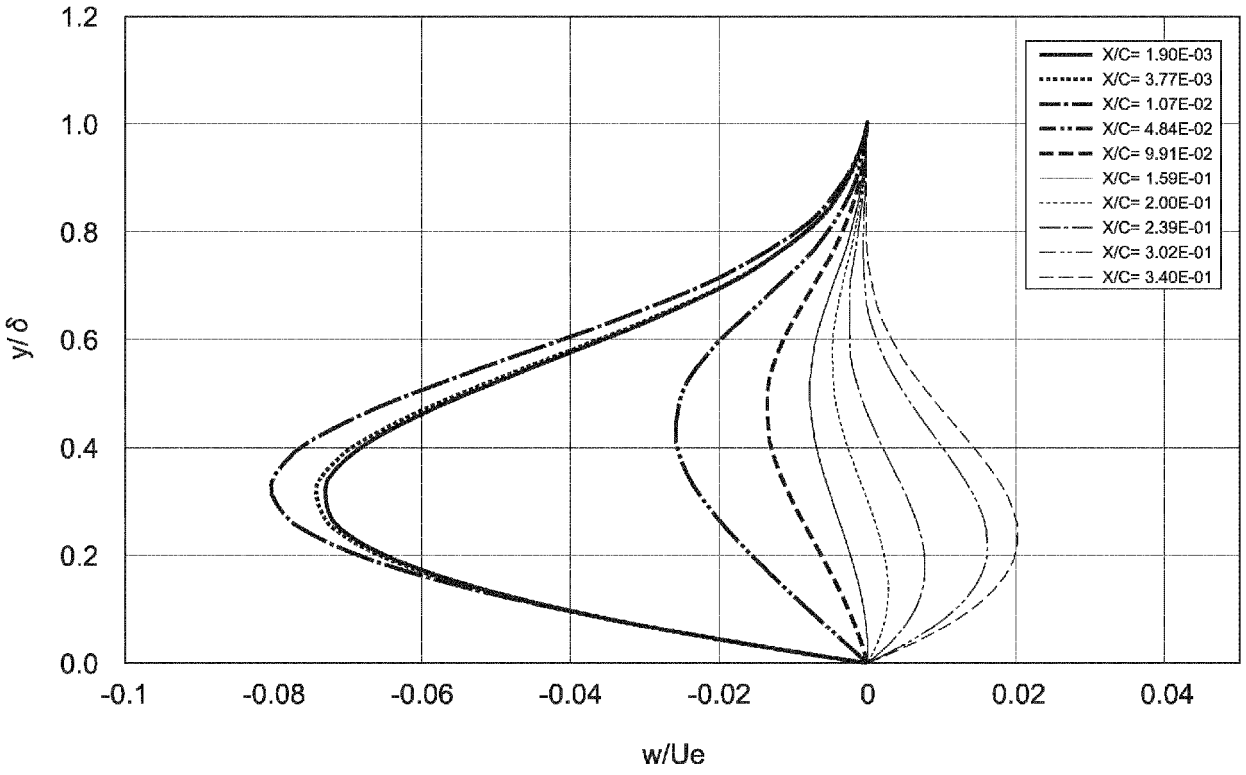
1.2
1.0
0.8
0.6
0.4
0.2
0.0
y/δ
-0.1
-0.08
-0.06
-0.04
-0.02
0
0.02
0.04
w/Ue
X/C= 1.90E-03
X/C= 3.77E-03
X/C= 1.07E-02
X/C= 4.84E-02
X/C= 9.91E-02
X/C= 1.59E-01
X/C= 2.00E-01
X/C= 2.39E-01
X/C= 3.02E-01
X/C= 3.40E-01

FIG.14

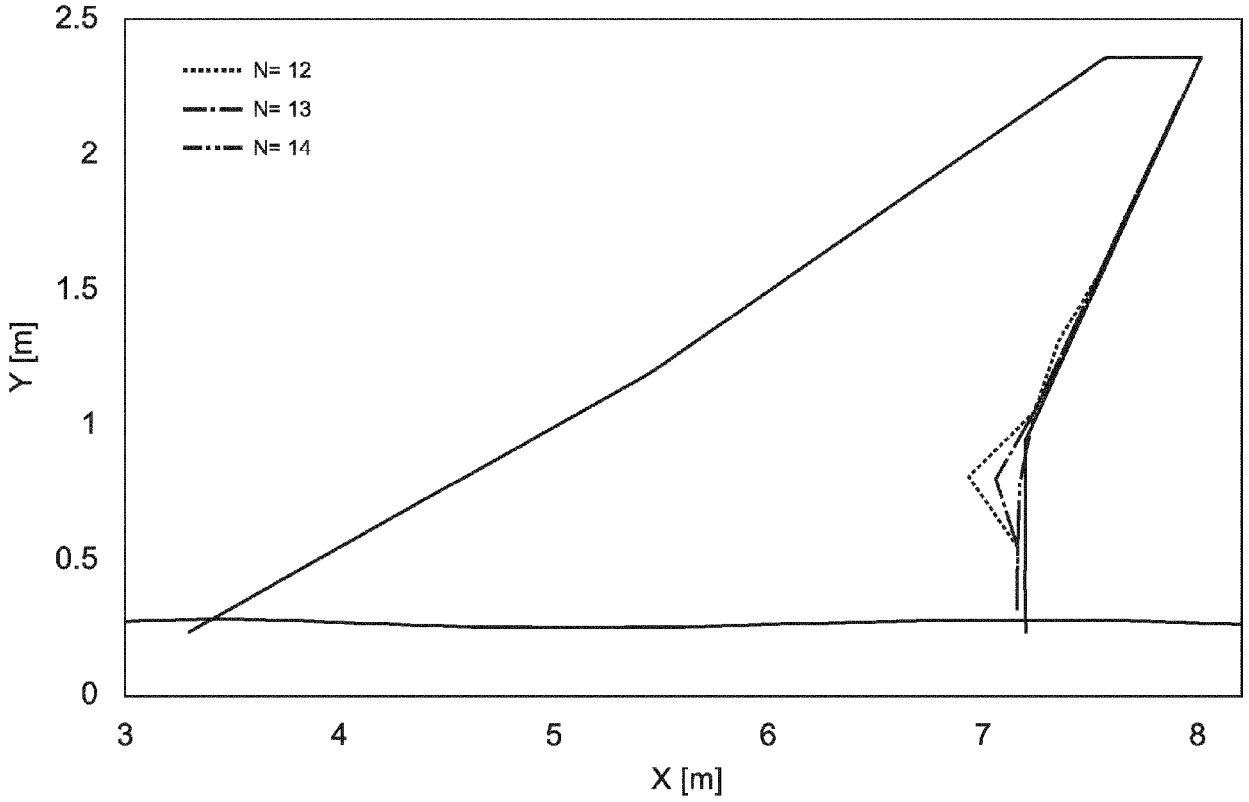

FIG.15

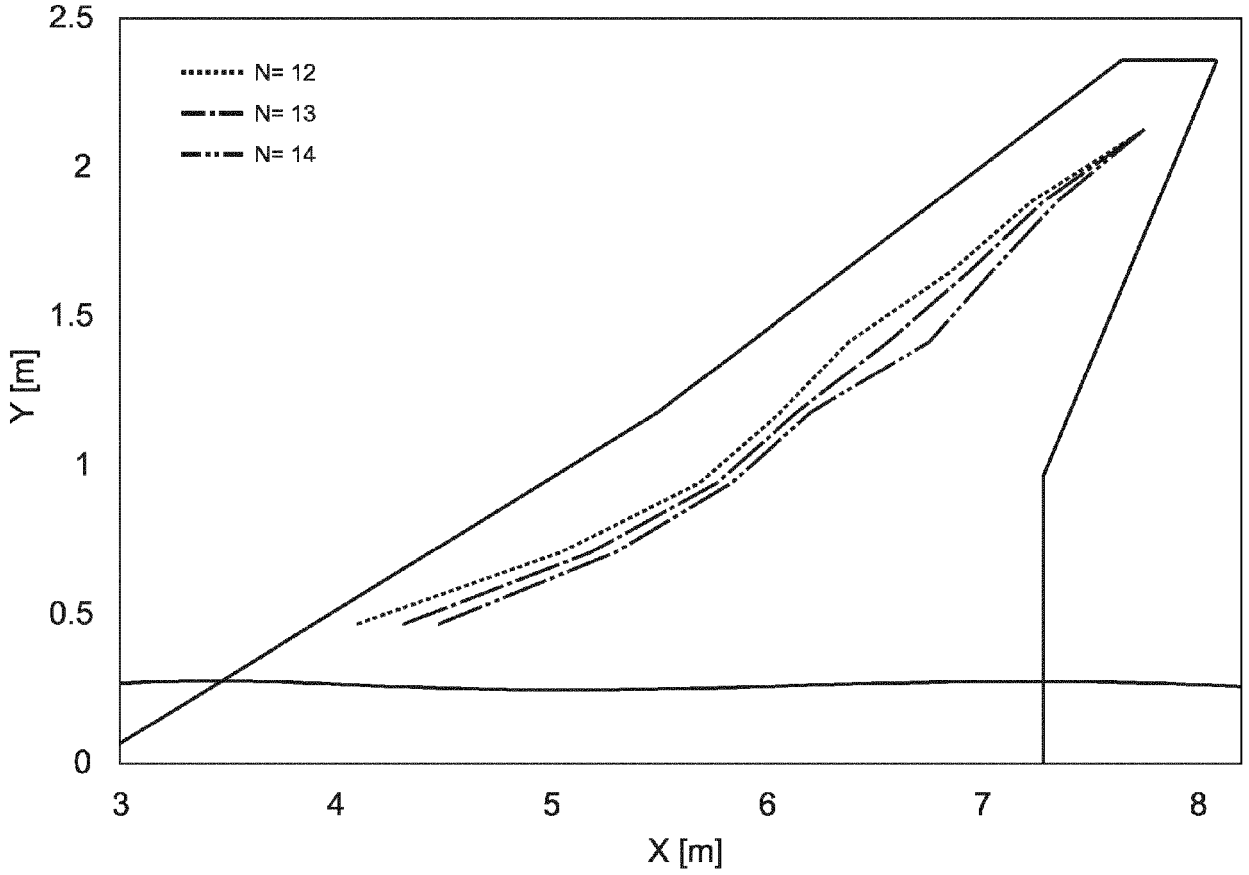

FIG.16

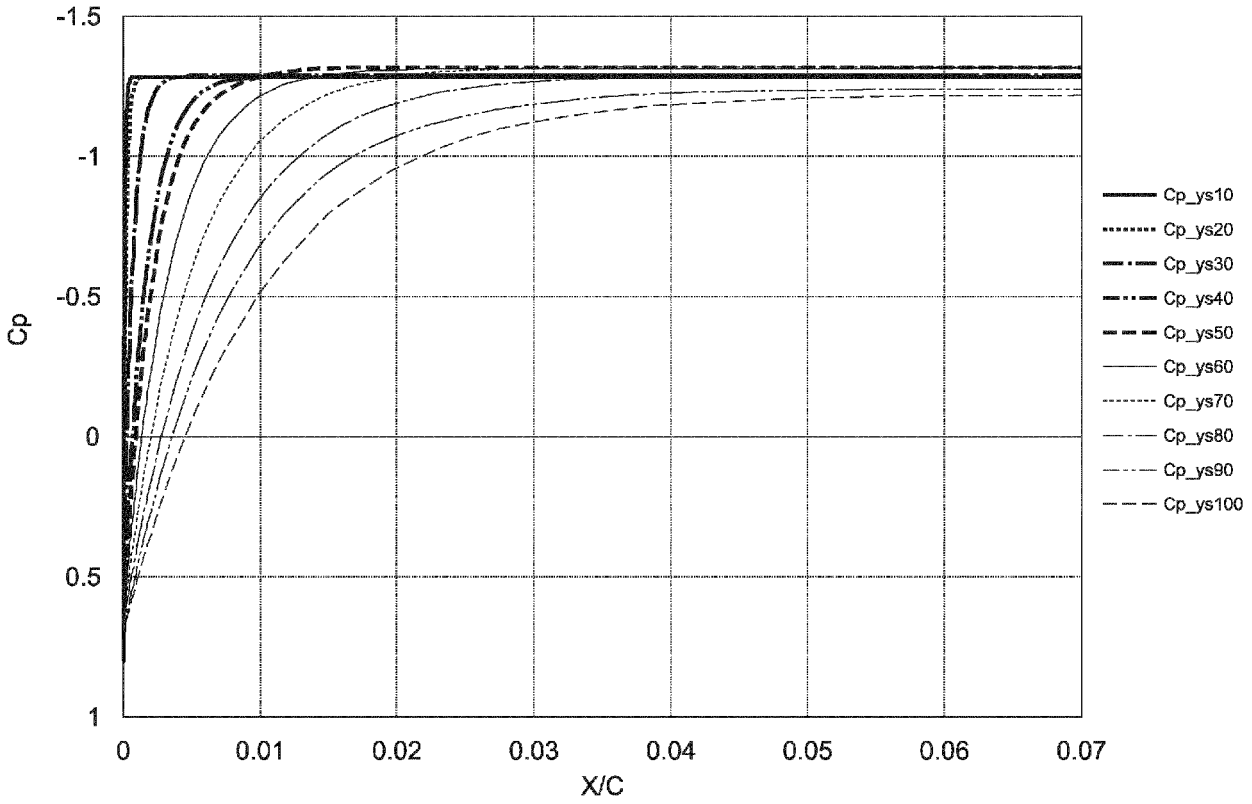
-1.5
-1
-0.5
0
0.5
1
Cp
0
0.01
0.02
0.03
0.04
0.05
0.06
0.07
X/C
Cp_ys10
Cp_ys20
Cp_ys30
Cp_ys40
Cp_ys50
Cp_ys60
Cp_ys70
Cp_ys80
Cp_ys90
Cp_ys100

FIG.17

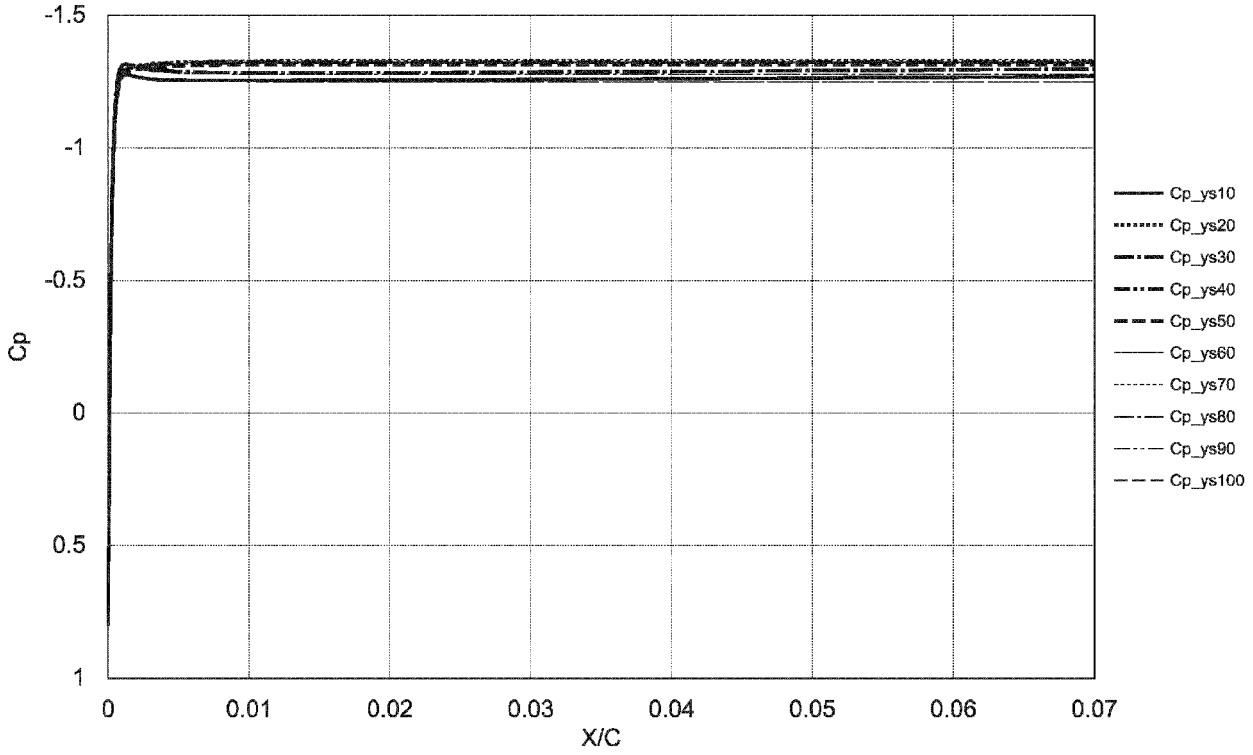
-1.5
-1
-0.5
0
0.5
1
Cp
0
0.01
0.02
0.03
0.04
0.05
0.06
0.07
X/C
Cp_ys10
Cp_ys20
Cp_ys30
Cp_ys40
Cp_ys50
Cp_ys60
Cp_ys70
Cp_ys80
Cp_ys90
Cp_ys100

FIG.18

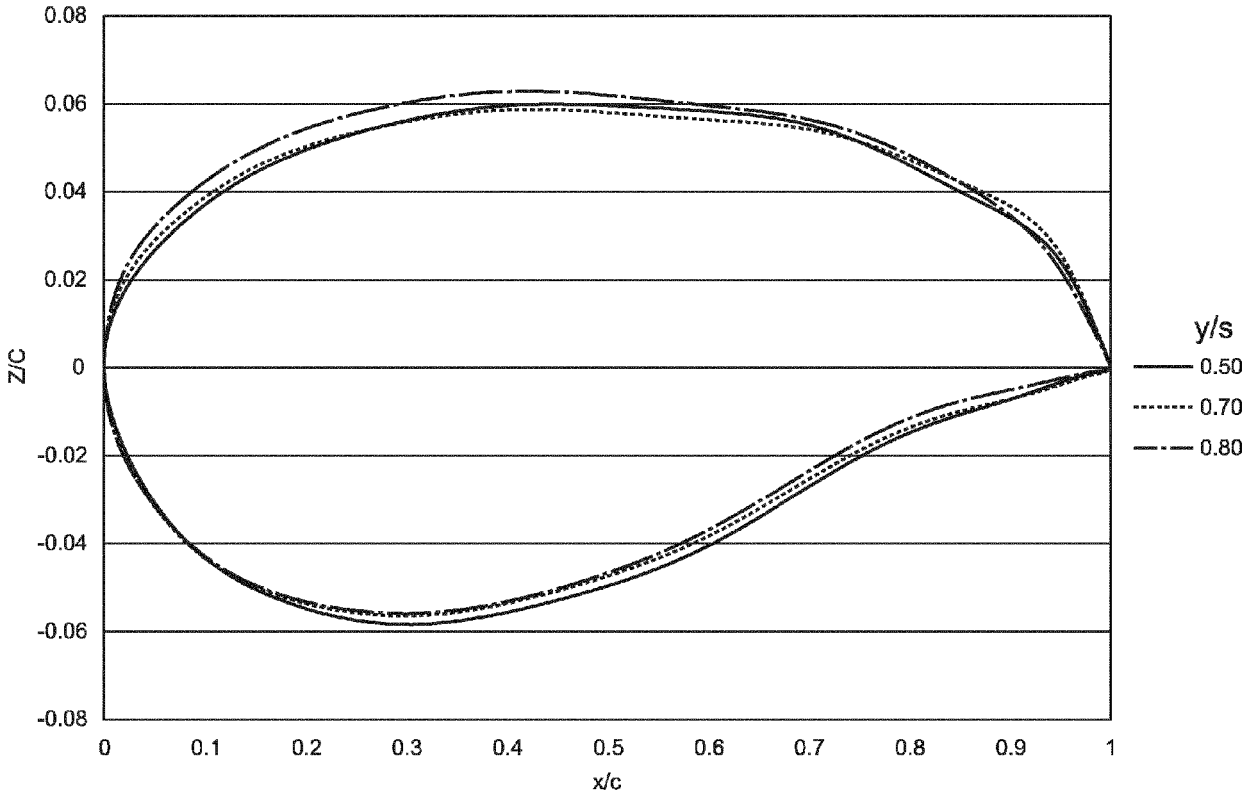
0.08
0.06
0.04
0.02
0
-0.02
-0.04
-0.06
-0.08
Z/C
0
0.1
0.2
0.3
0.4
0.5
0.6
0.7
0.8
0.9
1
x/c
y/s
0.50
0.70
0.80

FIG.19

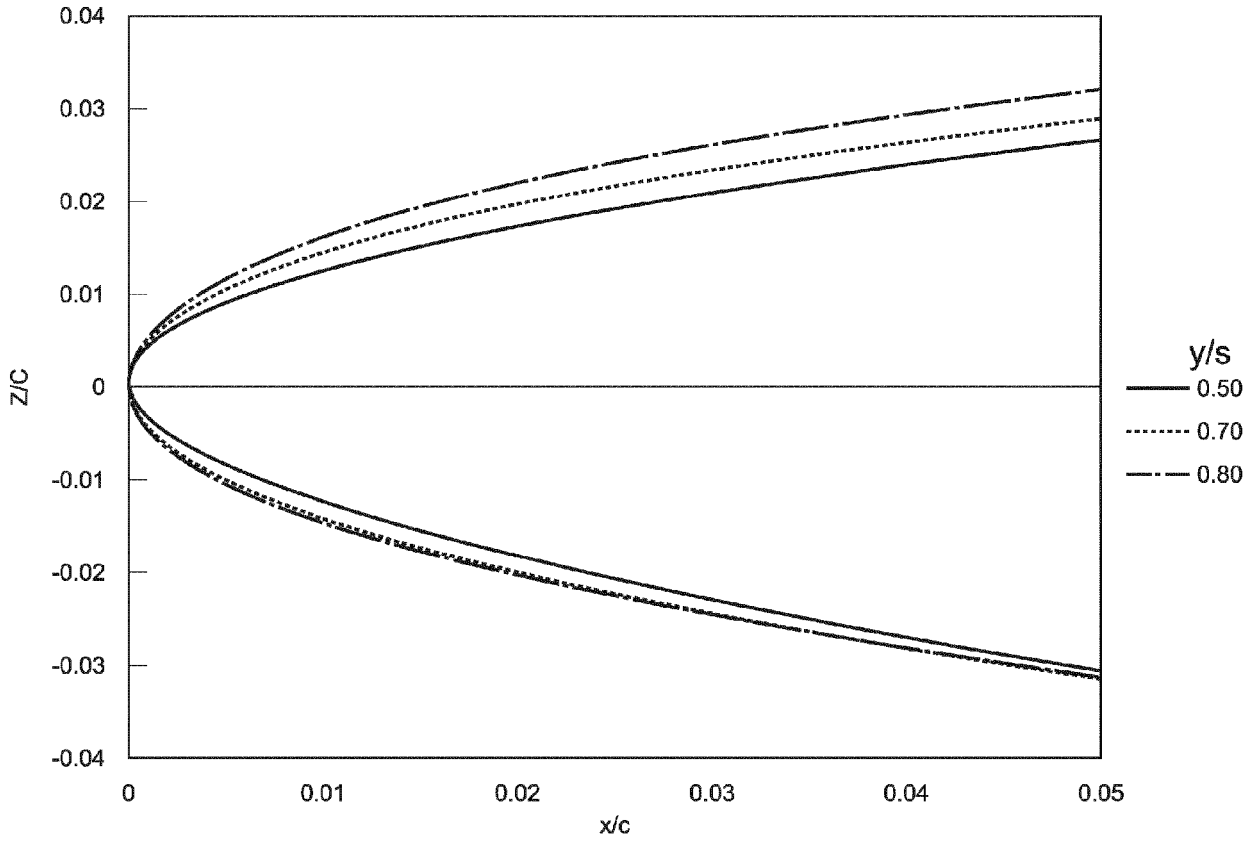
0.04
0.03
0.02
0.01
0
-0.01
-0.02
-0.03
-0.04
z/c
0
0.01
0.02
0.03
0.04
0.05
x/c
y/s
0.50
0.70
0.80

FIG.20

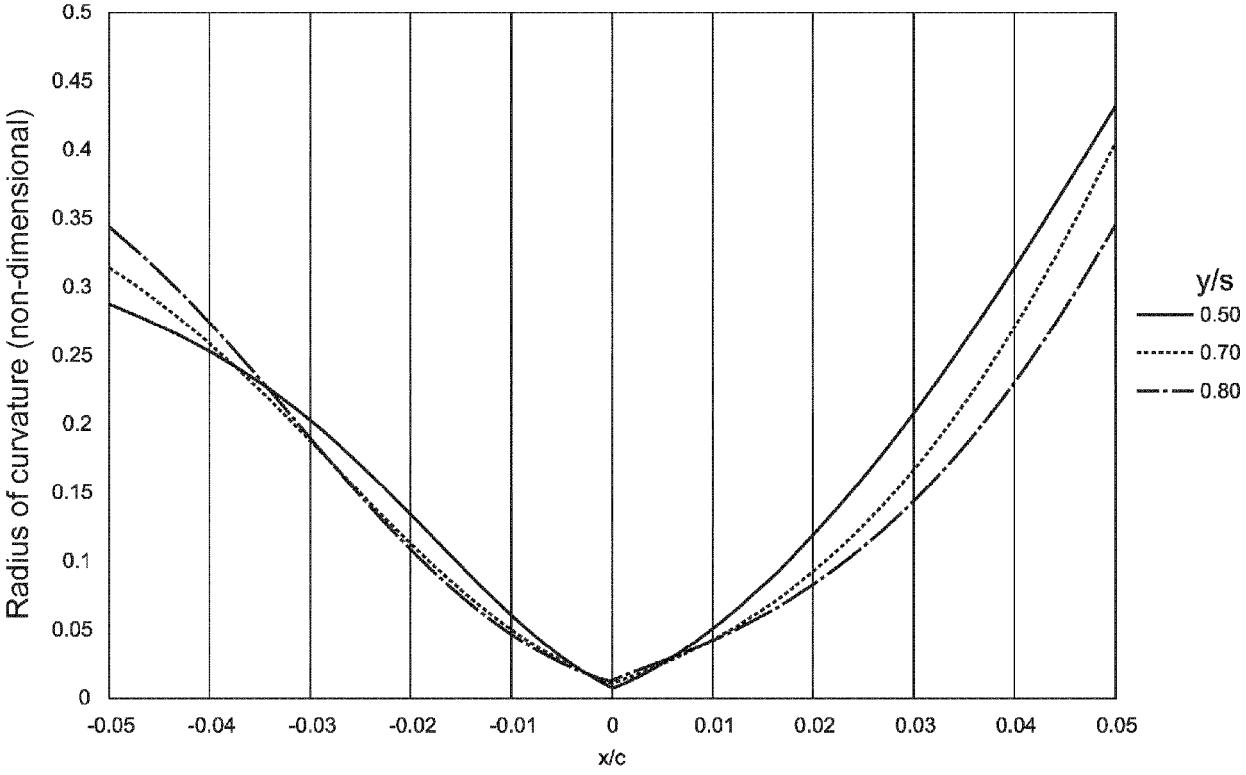
Radius of curvature (non-dimensional)
0.5
0.45
0.4
0.35
0.3
0.25
0.2
0.15
0.1
0.05
0
-0.05
-0.04
-0.03
-0.02
-0.01
0
0.01
0.02
0.03
0.04
0.05
x/c
y/s
0.50
0.70
0.80

FIG.21

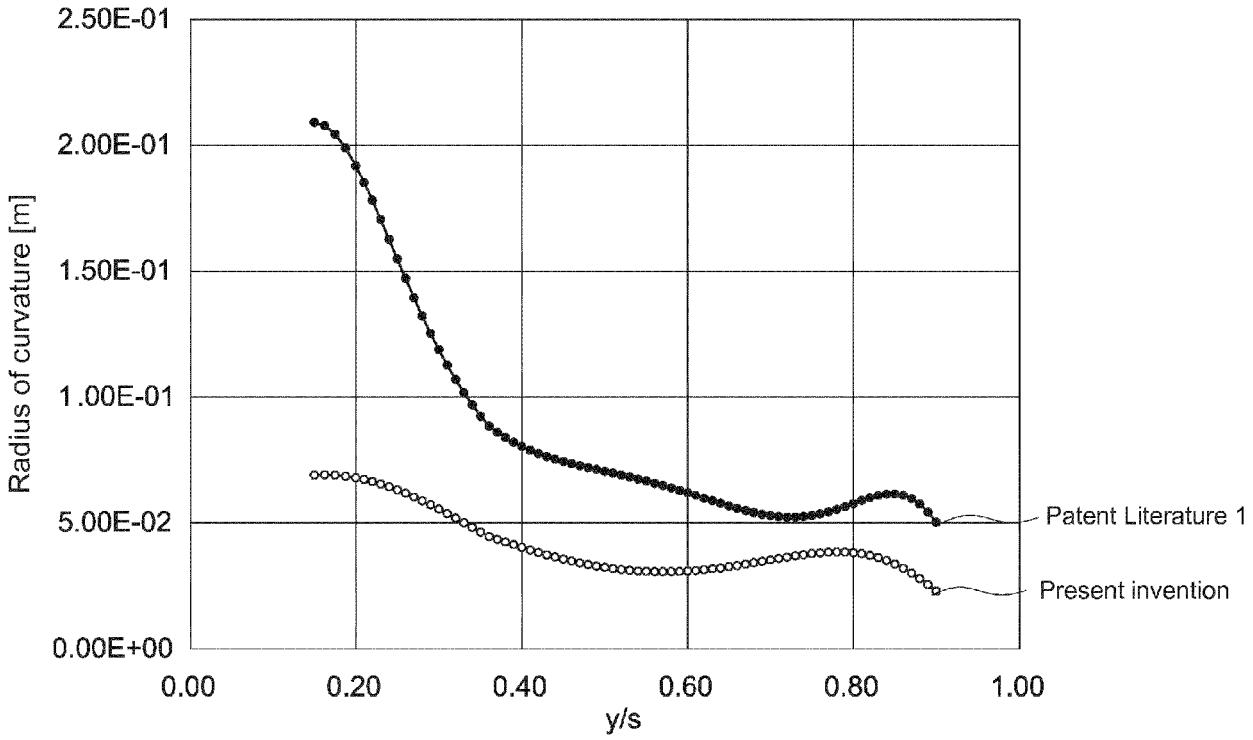
2.50E-01
2.00E-01
1.50E-01
1.00E-01
5.00E-02
0.00E+00
Radius of curvature [m]
0.00
0.20
0.40
0.60
0.80
1.00
y/s
Patent Literature 1
Present invention

FIG.22

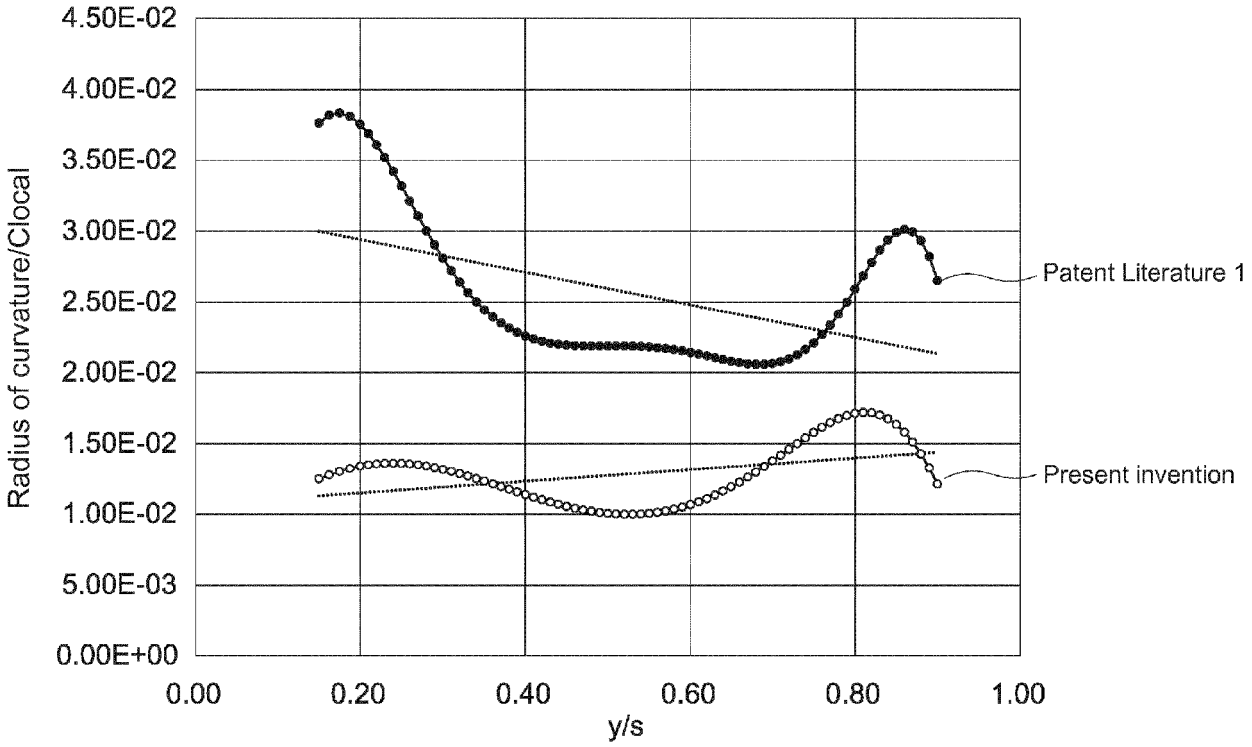
4.50E-02
4.00E-02
3.50E-02
3.00E-02
2.50E-02
2.00E-02
1.50E-02
1.00E-02
5.00E-03
0.00E+00
Radius of curvature/Clocal
0.00
0.20
0.40
0.60
0.80
1.00
y/s
Patent Literature 1
Present invention

FIG.23

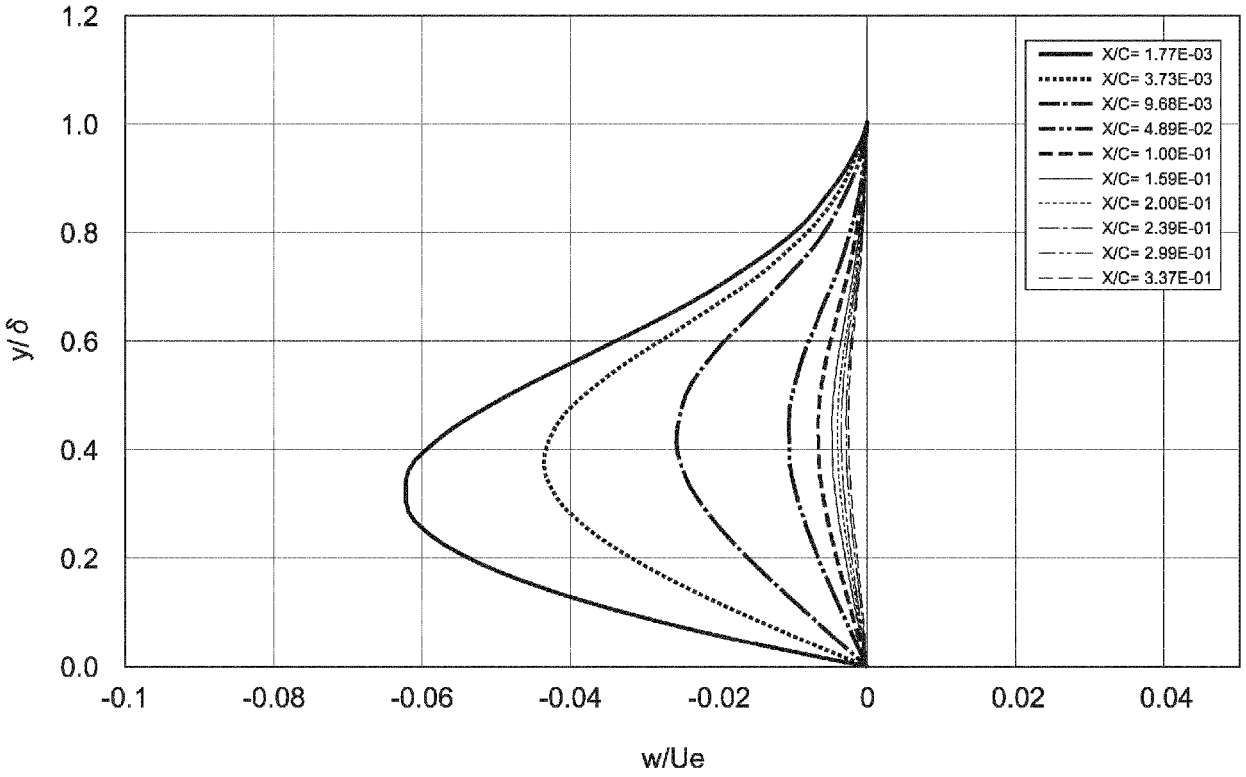
1.2
1.0
0.8
0.6
0.4
0.2
0.0
y/δ
-0.1
-0.08
-0.06
-0.04
-0.02
0
0.02
0.04
w/Ue
X/C= 1.77E-03
X/C= 3.73E-03
X/C= 9.68E-03
X/C= 4.89E-02
X/C= 1.00E-01
X/C= 1.59E-01
X/C= 2.00E-01
X/C= 2.39E-01
X/C= 2.99E-01
X/C= 3.37E-01

FIG.24

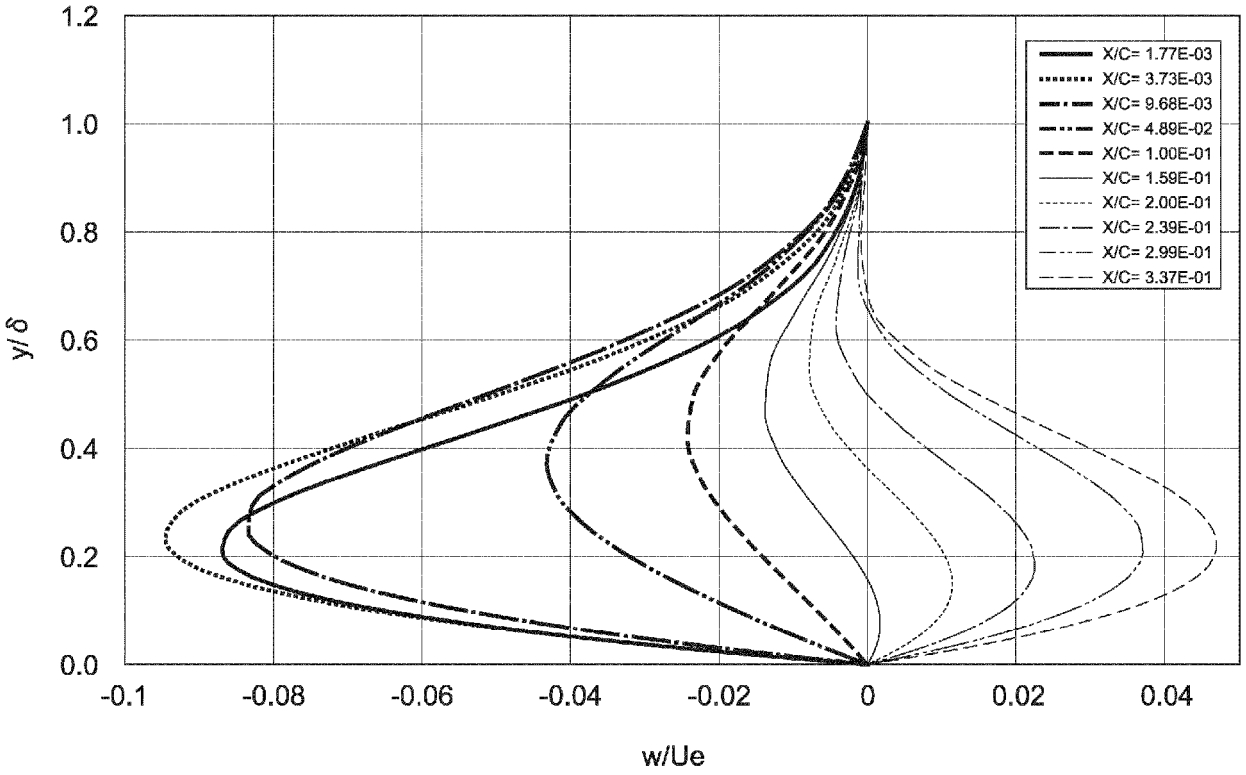
1.2
1.0
0.8
0.6
0.4
0.2
0.0
y/δ
-0.1
-0.08
-0.06
-0.04
-0.02
0
0.02
0.04
w/Ue
X/C= 1.77E-03
X/C= 3.73E-03
X/C= 9.68E-03
X/C= 4.89E-02
X/C= 1.00E-01
X/C= 1.59E-01
X/C= 2.00E-01
X/C= 2.39E-01
X/C= 2.99E-01
X/C= 3.37E-01

FIG.25

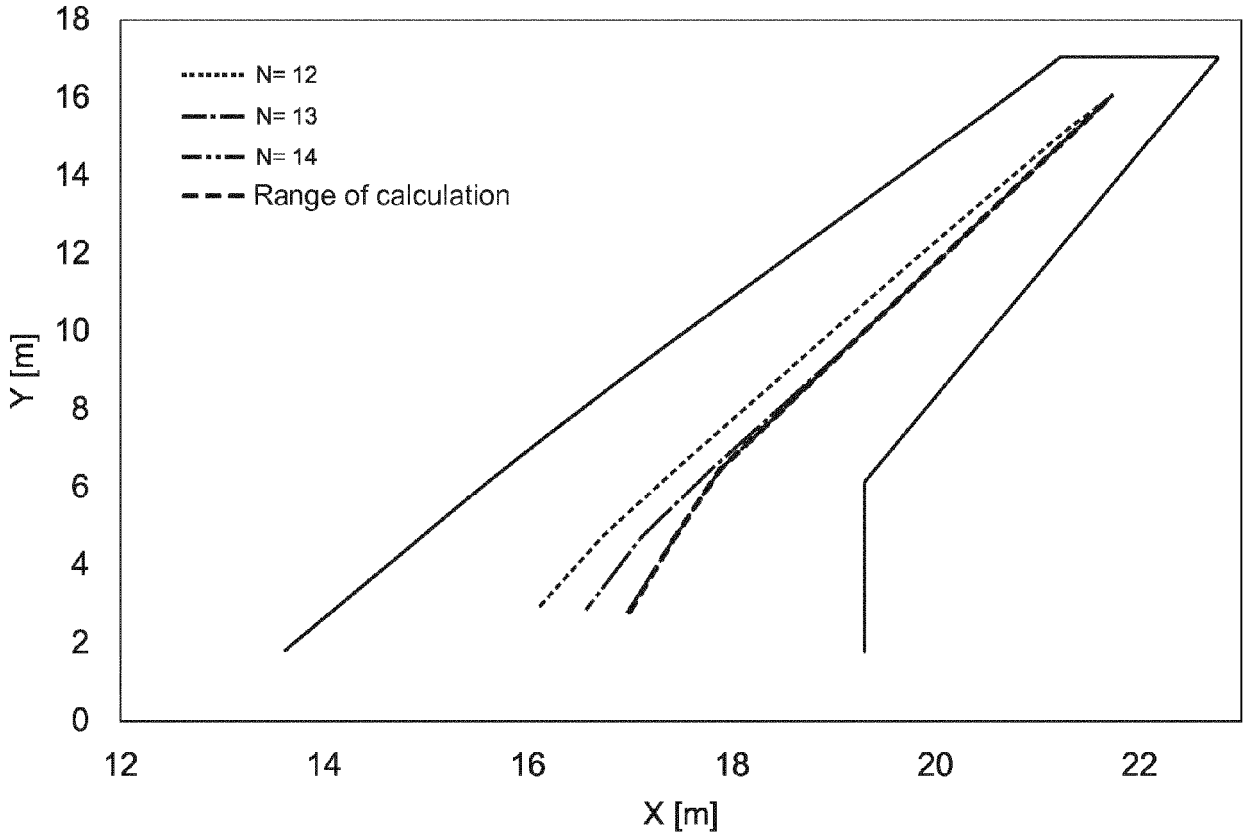
N= 12
N= 13
N= 14
Range of calculation
Y [m]
X [m]
0
2
4
6
8
10
12
14
16
18
12
14
16
18
20
22

FIG.26

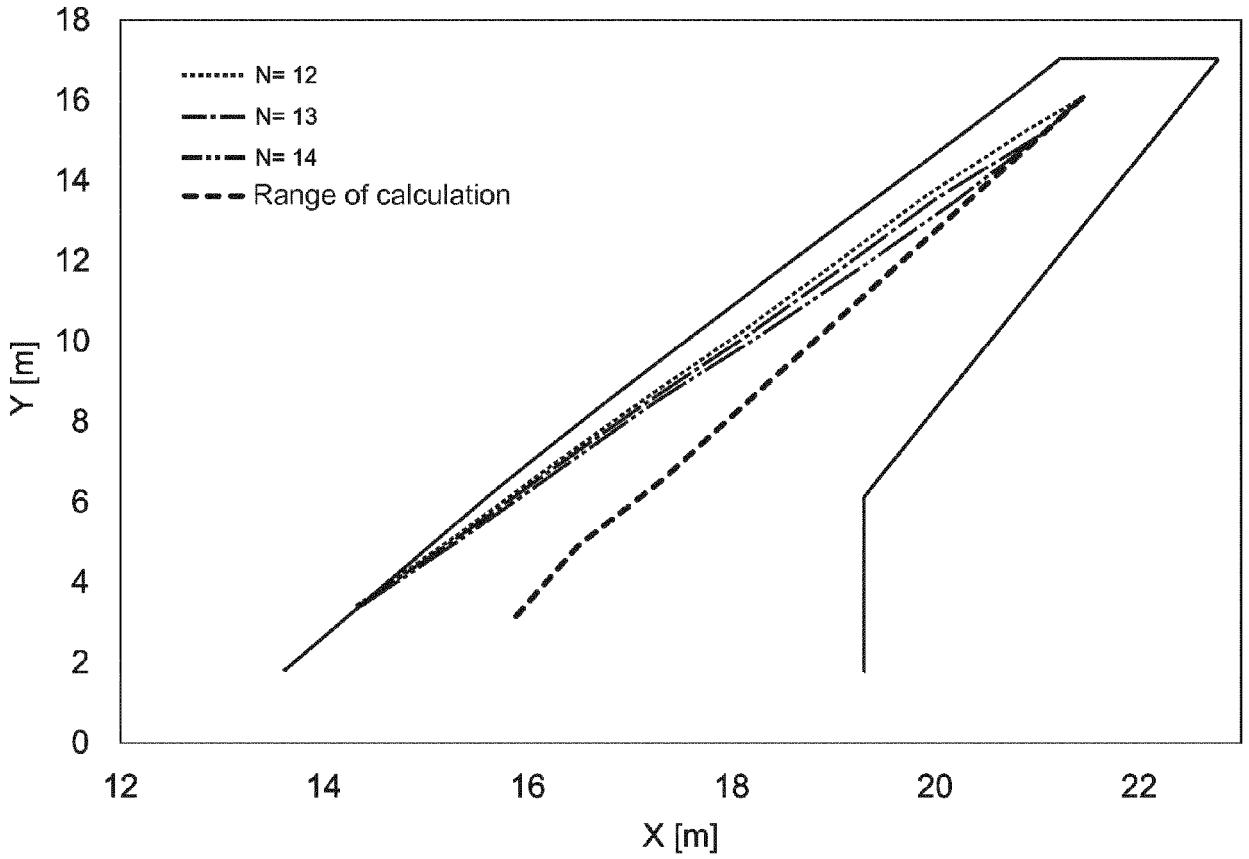
N= 12
N= 13
N= 14
Range of calculation
Y [m]
X [m]
0
2
4
6
8
10
12
14
16
18
12
14
16
18
20
22

FIG.27

REFERENCES CITED IN THE DESCRIPTION

This list of references cited by the applicant is for the reader's convenience only. It does not form part of the European patent document. Even though great care has been taken in compiling the references, errors or omissions cannot be excluded and the EPO disclaims all liability in this regard.

Patent documents cited in the description

- JP 5747343 B **[0006] [0031]**

Non-patent literature cited in the description

- **OLIVIER VERMEERSCH et al.** Natural laminar flow wing for supersonic conditions: Wind tunnel experiments, flight test and stability computations. *PROGRESS IN AEROSPACE SCIENCES,* vol. 79 **[0006]**
- **YOSHINE UEDA et al.** Supersonic Natural-Laminar-Flow Wing-Design Concept at High-Reynolds-Number Conditions. *AIAA JOURNAL,* vol. 52 (6 **[0006]**